



# The 9th International Electronic Conference on Medicinal Chemistry (ECMC 2023)

01–30 November 2023 | Online

## Quantitative relations among measurands of molecular isotopologies of halogenated pharmaceuticals – stochastic dynamic mass spectrometric approach

Chaired by **Dr. Alfredo Berzal-Herranz**  
and **Prof. Dr. Maria Emília Sousa**



*pharmaceuticals*



**Bojidarka Ivanova** <sup>1,\*</sup>

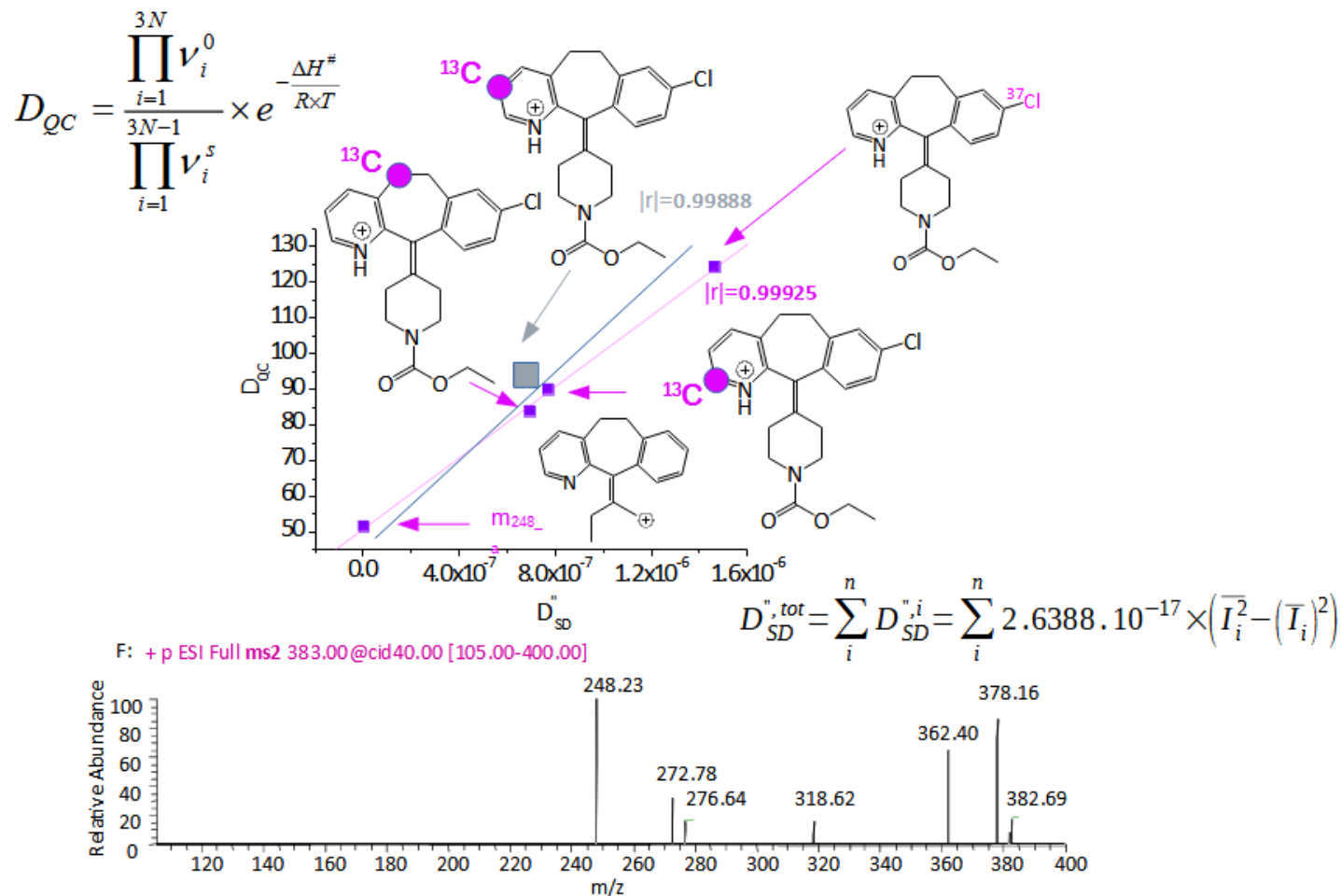
<sup>1</sup> Lehrstuhl für Analytische Chemie, Institut für Umweltforschung, Fakultät für Chemie und Chemische Biologie, Universität Dortmund, Otto-Hahn-Straße 6, 44221 Dortmund, Nordrhein-Westfalen, Deutschland.

\* Corresponding author: [bojidarka.ivanova@yahoo.com]; [b\_ivanova@web.de]



## Quantitative relations among measurands of molecular isotopologues of halogenated pharmaceuticals – stochastic dynamic mass spectrometric approach

### Graphical Abstract





## Abstract:

The paper serves two goals. Its first aim is to approach *mass spectrometric* measurands such as mass-to-charge ( $m/z$ ) and peak intensity variables of *molecular isotopologies* of halogenated pharmaceuticals diclofenac (1) and loratadine (2) with respect to conditions of measurements, involving collision energy and concentration of presented formic acid; if any, *via* our stochastic dynamic model equation [**equation 2**]. In addition, it is tested its most recently derivative formulas [**equation 4**] and [**equation 5**], connecting among experimental measurands with respect to experimental conditions, particularly, accounting for collision energy and concentration of formic acid. So far, the latter equations have been tested on two molecular models of labetalol and acetaminophen. Secondly, the first shown equation is used to determine 3D molecular and electronic structures of analytes, mass spectrometrically. The task is carried out *via* its complementary application to Arrhenius's equation. Those two domains constitutes fundamental background of the *analytical mass spectrometry*, consisting in analyte quantitative and 3D structural analyses, which are approaches only using one and the same stochastic dynamic equation. There are utilized ultra-high resolution electrospray ionization mass spectrometric data in addition to high accuracy quantum chemical static methods and molecular dynamics. Tests of *chemometrics* are used, as well.

**Keywords:** Mass spectrometry ; stochastic dynamics ; molecular isotopologies ; pharmaceuticals



$$D_{SD}^{tot} = \sum_i^n D_{SD}^i = \sum_i^n 1.3194 \cdot 10^{-17} \times A^i \times \frac{\overline{I}_i^2 - (\overline{I}_i)^2}{(I_i - \overline{I}_i)^2} \quad \text{Equation (1)}$$

$$D_{SD}^{",tot} = \sum_i^n D_{SD}^{",i} = \sum_i^n 2.6388 \cdot 10^{-17} \times (\overline{I}_i^2 - (\overline{I}_i)^2) \quad \text{Equation (2)}$$

$$D_{QC} = \frac{\prod_{i=1}^{3N} \nu_i^0}{\prod_{i=1}^{3N-1} \nu_i^S} \times e^{-\frac{\Delta H^\ddagger}{R \times T}} \quad \text{Equation (3)}$$

$$\overline{I}^{TOT,q} = \frac{1}{2} \times \frac{A_I^q}{A_D^q} \times D_{SD}^{",q} \quad \text{Equation (4)}$$

$$D_{SD,l}^{"} + D_{SD,m}^{"} = |r_{l,m}| \times \sqrt{\overline{I}_{l,q}^2 - (\overline{I}_{l,q})^2} \times \sqrt{\overline{I}_{m,q}^2 - (\overline{I}_{m,q})^2} \quad \text{Equation (5)}$$



## Introduction

Various *-omics-methods* (*lipidomics; metabolomics; proteomics, including (neuro)-proteomics; foodomics; steroidomics; pesticide analysis and control; glycomics; genomics and DNA adductomics; lignomics; genomics, transcriptomics, interactomics; clinical trans-omics; doping control; petroloomics; isotomics; and more*) have widespread application to *mass spectrometry (MS)* [1–3]. They have gained importance in studying chemistry of biological systems. *Bioinformatics* is mainly governed, in fact, by MS based *bioanalytical approaches* [3]. *Metabolomics*, is based on hyphenated instrumentation of LC-MS<sup>n</sup> [4,5]. Its databases can be complex and chemically heterogeneous; thus, causing for a challenge to determine reliably structurally similar metabolites; enantiomers; isomers; or molecular *isotopologies*, respectively. Identification of LMWs is associated with significant error. *Metabolomics* databases often show relatively low reproducibility of measurands among instrumentation and laboratories; also, a great variability of data-quality. Therefore, structural elucidation of LMWs and reliability of both quantitative and structural analyses are challenging research tasks; strictly speaking - errors occur. The *molecular annotation* is carried out *via* tasks involving: (i) Conversion of measurands; (ii) peak detection and (iii) alignment; (iv) correction of retention time; (v) detection of isotopes, including molecular isotopologies; (vi) annotation of MS adducts; if any; (vii) annotation of peaks, and (viii) data-processing of measurands [4–7]. Molecular structural information is gained *via* tandem operation MS<sup>n</sup> mode. However, under term *annotation* there is understood a putative association of a molecule to its structure [4], or a rather deduction of analyte molecular structure. It is very far from chemical term *3D molecular structure* [8]. It assumes determination of 3D molecular geometry parameters and electronic structures of analytes.

Further: What there might be termed *molecular identification* is focused on confirmation of annotated molecular structure with metabolic standard; if any [4]. Often, this is a drawback to *-omics-methods*. Even in cases, when there are standard reference spectra of analytes, we shall turn to comment on made above that neither annotated nor identified 2D molecular structure provide crucial for the chemistry 3D molecular geometries and electronic structures. Arguments for maintaining the later position has been shown [8].

Furthermore, we could make point in that task of *molecular annotation* is frequently a manual process. Selection of best candidate among a set of possible molecular structures which is significantly time and labour consuming research effort [4–7].

Despite, for deduction of 2D molecular structure of analyte among a large number of metabolites of biological or environmental samples application of *-omics-methods* is sufficient as a first analytical stage. However, detail understanding on chemistry of molecules, particularly examining chiral compounds, in addition to their chemical reactivity, the second stage of 3D structural determination of molecular conformation and electron density distribution of atoms in molecules is crucial task. At this point, the readers shall be recalled that we have returned their attention on issue of methodological development of exact MS methods for quantitative and 3D structural analyses. A central issue is whether there is approach capable of serving at both quantitative and structural research tasks of *analytical mass spectrometry*. A seemingly very plausible strategy of solving the latter problem appears equations (1) and (2), quantifying *fluctuations* of MS measurands *per* short spans of scan time [9–15]. As we saw in contributions devoted to the issue, so far, equation (2) which is derived from equation (1) appears exact model for quantifying analytes mass spectrometrically.



# The 9th International Electronic Conference on Medicinal Chemistry

01–30 November 2023 | Online



In practice, complementary employment in equation (2) and Arrhenius's equation (3) provides exact 3D molecular and electronic structures; thus, allowing us not only to determine analyte quantitatively, but also 3D structurally, using formula (2). *Chemometrics* of correlation of data on equations (2) and (3) has shown  $r=1-0.9833$  [13,16]. Equation (2) is capable of assigning subtle electronic effects of tautomers, showing  $|r|=1$  [13,14]. It is applicable to complex environmental and foodstuff samples in addition to biological fluids [8,14].

Equation (2) has been tested on soft ionization MS methods and technique such as ESI, APCI, MALDI, CID, HCD, and UVPD [8–18], quantifying results from  $MS^2$ – $MS^7$  operation modes under positive and negative polarities [15,17]. Equation (2) has been justified correlating MS and chromatographic data on steroids. The chromatographic analysis shows  $|r|=0.9991_4$ , while MS quantitation according to equation (2) leads to  $|r|=0.9999_4$  [12]. Equation (2) processes measurands from hard ionization MS methods, as well [19,20]. An assessing on its advantages has revealed a problem, however. It is an exact MS law obeyed by temporal distribution of measurand intensity of MS peak *per* any span of scan time, however, is applicable to a certain set of experimental conditions. In solving this problem we have further derived equations (4) and (5) from equations (1) and (2), thus writing innovative models capable of quantifying measurands of any two set of experimental conditions of measurements accounting for experimental factors such as collision energy, infusion volumes, and more [14,15,17].

Perhaps, there is created impression that equations (1), (2), (4) and (5) have already practical bearing, but that it is far from being the case. The capability of equations (1) and (2) for exact quantitative and structural analyses has been tested on a number of molecules and *chemometric* data have been reviewed [16,20]. Despite, many important for the field of chemistry research problems are still not addressed. An example is determination of *molecular isotopologies*. Furthermore, equations (4) and (5) have been tested, so far, on only two molecular objects [8,15], showing  $|r|=0.9997_2-0.99999$  of CID- $MS^7$  spectra of labetalol [15]. However, a lack of a statistically representative set of tested molecules unable us to assess risk to which those formulas may be regarded as universally applicable ones to purposes of *analytical mass spectrometry*. Thus, most striking empirical justification of statement that as equation (2), formulas (4) and (5) are also universal MS laws may be provided by a systematic examining of a set of molecular objects and samples, having complex matrix effects. Part of our effort in addressing the issue is this study, dealing with quantitation of isotopologies of diclofenac (1) and loratadine (2) *via* formulas (1), (2), (4) and (5) in addition to determine their 3D molecular and electronic structures using complementarily equations (2) and (3). Pharmaceuticals (1) and (2) exhibit distinctive isotope patterns of ions, due to chlorine atom(s), causing for MS isotope shape components exhibiting difference of  $m/z$  values  $\Delta(m/z)=1$  and 2 of  $^{13}C$  and  $^{37}C$ -isotopes. The study refers to determine isotope specific positions. New empirical proofs of great capability of formula (2) to quantify exactly isotope specific positions of  $^{13}C$ -isotopes are vigorously deployed, since, as can be expected looking at chemical diagrams of analytes (1) and (2) there is little affect on molecular properties from positions of  $^{13}C$ -isotope of aromatic fragments. The claim about distinctive capability of equation (2) of determining subtle electronic effects and isotope specific positions examining MS measurands and high accuracy quantum chemical data on electronic structures of analytes which is proven empirically in this study, thereby, extends capability of our model formulas, and experimental mass spectrometry as a robust analytical method for not only exact determination of analytes, but also their 3D conformational and electronic structural analyses.



There are issues in the study which play crucial role in research devoted to *analytical mass spectrometry*. The method has a many applications, ranging from environmental quality control monitoring; food control; clinical diagnostics; and medicine, respectively. The most important of these issues is that the innovative method presented, herein, provides exact quantification of the *fluctuations* of experimental variable intensity of analyte MS peak; furthermore, accounting for sub-peaks of isotope patterns. We shall draw on important most recent application of isotope ratio to quantitative mass spectrometry. The determination of isotope ratio of chlorine adducts of sialic acid of N-linked glycans has been used to develop MS based method for determination of content of sialic acid. Changes in sialylation of glycans as a tumor marker are associated with various types of cancer, in addition to cardiovascular disease and genetic disorders [21]. The <sup>13</sup>C- and <sup>15</sup>N-isotope ratio is used to develop MS method for determining smokeless powder in improvised explosive devices for purposes of forensic science and anti-terrorism activities [22]. Therefore, methodological developments of exact methods for MS data-processing of measurands is highly justifiable, due to broad practical interdisciplinary applications of the *mass spectrometry* to different fields of fundamental science, industry, and control authorities, respectively.

## Experimental

The contribution has used experimental MS database on MS measurements available in [23,24].

[<https://doi.org/10.5281/zenodo.6543678>] [<https://doi.org/10.5281/zenodo.6545447>]

- [1] S. Sugar, L. Drahos, K. Vekey, *J Mass Spectrom.* 58 (2023) e4907.
- [2] F. Chen, W. Chen, Z. Wang, Y. Peng, B. Wang, B. Pan, W. Guo, *J. Mass Spectrom. Adv. Clin. Lab* 29 (2023) 2–8.
- [3] F. Hormann, S. Sommer, S. Heiles, *J. Am. Soc. Mass Spectrom* (2023) [<https://doi.org/10.1021/jasms.3c00126>].
- [4] M. Zulfiqar, L. Gadelha, C. Steinbeck, M. Sorokina, K. Peters, *J. Cheminform.* 15 (2023) 32.
- [5] R. Samples, S. Puckett, M. Balunas, *Anal. Chem.* 95 (2023) 8770–8779.
- [6] A. Bilbao, et al. *Nat. Commun.* 14 (2023) 2461.
- [7] L. Huang, Q. Shan, Q. Lyu, S. Zhang, L. Wang, G. Gao, *Anal. Chem.* (2023) DOI: [10.1021/acs.analchem.3c01072]
- [8] B. Ivanova, *Int. J. Mol. Sci.* 24 (2023) 6306.
- [9] B. Ivanova, M. Spiteller, *Steroids* 181 (2022) 109001.
- [10] B. Ivanova, M. Spiteller, Experimental mass spectrometric and theoretical treatment of the effect of protonation on the 3D molecular and electronic structures of low molecular weight organics and metal–organics of silver(I) ion, In book: *Protonation: Properties, Applications and Effects*, A. Germogen (Ed.) (2019), Nova Science Publishers, N.Y., pp. 1–182, ISBN: 978-1-53614-886-2.
- [11] B. Ivanova, M. Spiteller, *Anal. Chem. Lett.* 10 (2020) 703–721.
- [12] B. Ivanova, M. Spiteller, *Steroids* 164 (2020) 108750.
- [13] B. Ivanova, M. Spiteller, Chapter 1: Mass spectrometric and quantum chemical treatments of molecular and ionic interactions of a flavonoid-O-glycoside – A stochastic dynamic approach, in *Advances in Chemistry Research*, Vol. 74, J. Taylor (Ed.) NOVA Science Publishers, New York (2022) pp. 1–126.



# Results and discussion

## 1. Mass spectrometric data

ESI-MS spectra of analytes (1) and (2) are depicted in **Figures 1** and **2**. **Figures 3** and **4** depict their fragmentation schemes. Fragmentation reactions of (1) depending on conditions of MS measurements are discussed [25–32]. The GC-SIM-MS analysis of (1) is based on fragmentation reaction: ( $m/z$  318;  $[M+Na]^+$ ) 214 (100); 242 (70); 277 (50) [25]. Data on relative abundance of fragmentation ions [%] are show in parentheses.

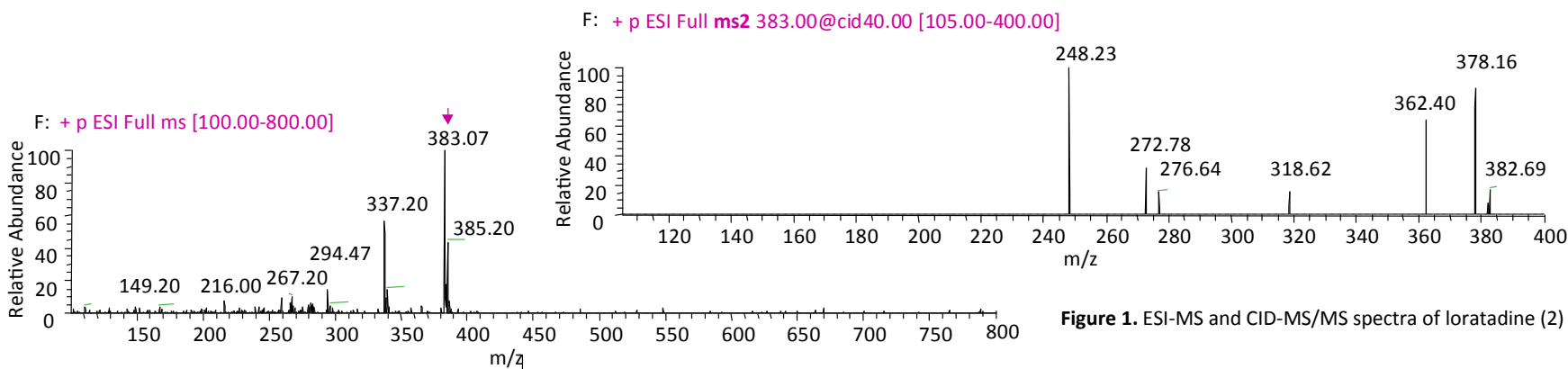


Figure 1. ESI-MS and CID-MS/MS spectra of loratadine (2)

[14] B. Ivanova, M. Spiteller. *Anal. Chem. Lett.* 12 (2022) 322–348.

[15] B. Ivanova, M. Spiteller, *Anal. Chem. Lett.* 12 (2022) 542–561.

[16] B. Ivanova, M. Spiteller, *Rev. Anal. Chem.* 38 (2019) 20190003 [10.1515/revac-2019-0003].

[17] B. Ivanova, M. Spiteller, *Environ. Sci. Poll. Res.* (2023) [https://doi.org/10.1007/s11356-022-24259-z]

[18] B. Ivanova, M. Spiteller, *J. Mol. Struct.* 1260 (2022) 132701.

[19] B. Ivanova, M. Spiteller *SSRN e Journal* (2023) [https://dx.doi.org/10.2139/ssrn.4334866].

[20] B. Ivanova, M. Spiteller, *Stochastic dynamics hard- and soft-ionization mass spectrometry*,

GRIN Verlag, Muenchen (2023) ISBN: 9783346835482.

[21] T. Palomino, D. Muddiman, *J. Am. Soc. Mass Spectrom.* (2023) [https://doi.org/10.1021/jasms.3c00100].

[22] S. Hlohowskyj, K. Kew, L. Stern, C. Yamnitz, *J. Am. Soc. Mass Spectrom.* (2023) [https://doi.org/10.1021/jasms.3c00047].

[23] R. Townsend, A. Godfrey, G. van Keulen, Geertje, G. Brenton, *Mass spectrometric investigation of pharmaceuticals in environmental matrices – homogenate analysis: Thesis Data 1 [Data set]; Zenodo* (2022) [https://doi.org/10.5281/zenodo.6543678].

[24] R. Townsend, A. Godfrey, G. van Keulen, Geertje, *Mass spectrometric investigation of pharmaceuticals in environmental matrices – homogenate analysis: Thesis Data 2 [Data set]; Zenodo* (2022) [https://doi.org/10.5281/zenodo.6545447].

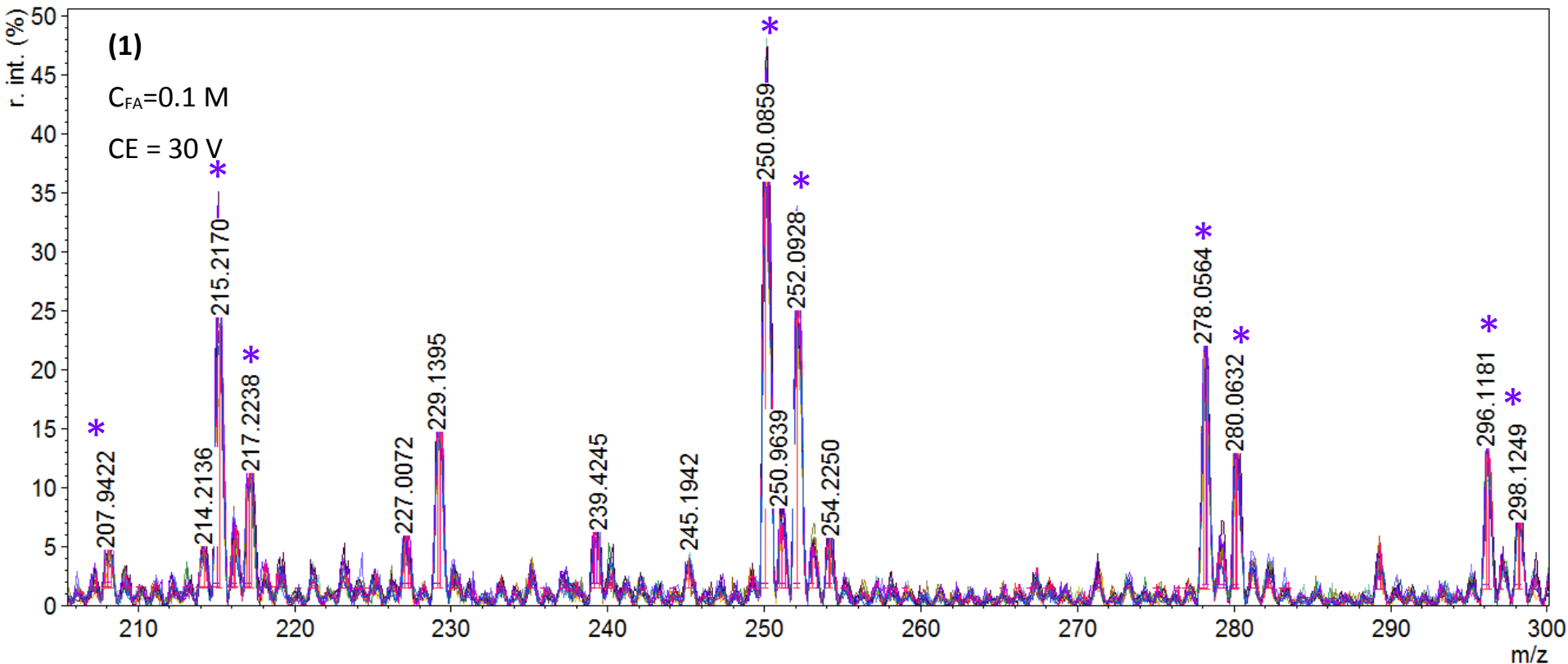


**Figure 2.** ESI-MS spectra of diclofenac (1) per short span of scan time and at presence of formic acid ( $C_{FA} = 0.1 \text{ M}$ ) and collision energy  $CE = 30 \text{ V}$ .

[25] M. Galmier, B. Bouchon, J. Madelmont, F. Mercier, F. Pilotaz, C. Lartigue, J. Pharmaceut. Biomed. Anal. 38 (2005) 790–796.

[26] T. Kosjek, D. Zigon, B. Kralj, E. Heath, J. Chromatogr. A, 1215 (2008) 57–63.

[27] M. Gomez, M. Bueno, S. Lacorte, A. Fernandez-Alba, A. Agueera, Chemosphere 66 (2007) 993–1002.

[28] I. Ferrer, E. Thurman, Anal. Chem. 77 (2005) 3394–3400.

[29] S. Perez, D. Barcelo, Anal. Chem. 80 (2008) 8135–8145.

[30] L. Minetto, F. Mayer, C. Mallmann, A. Martins, 40 (2012) 950–957.

[31] S. Wilkinson, S. Martin, A. Orton, R. Markandu, B. Jones, Rapid Commun Mass Spectrom. 34 (2020) e8735.

[32] I. Ivshina, E. Tyumina, M. Kuzmina, E. Vikhareva, Sci. Rep 9 (2019) 9159.

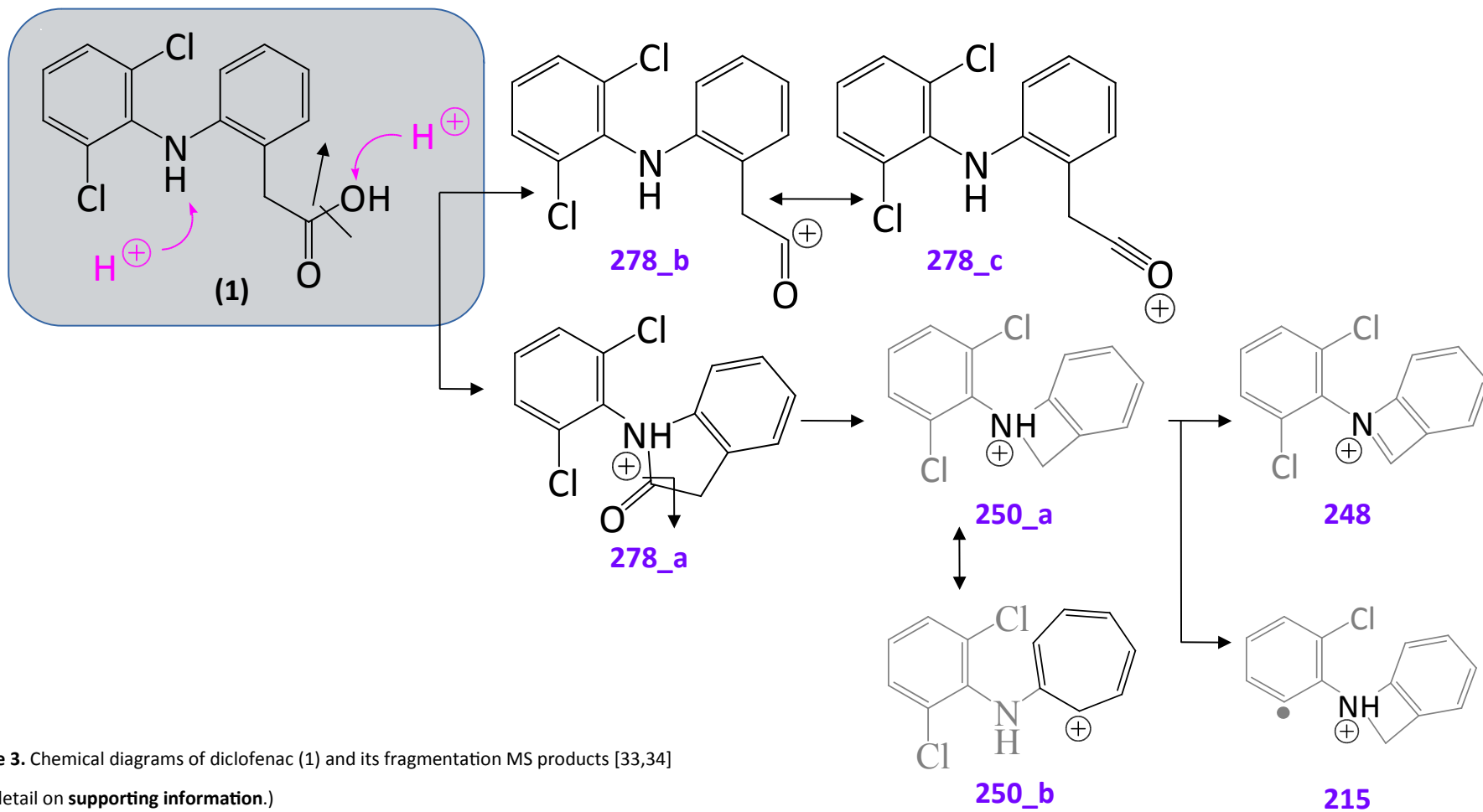
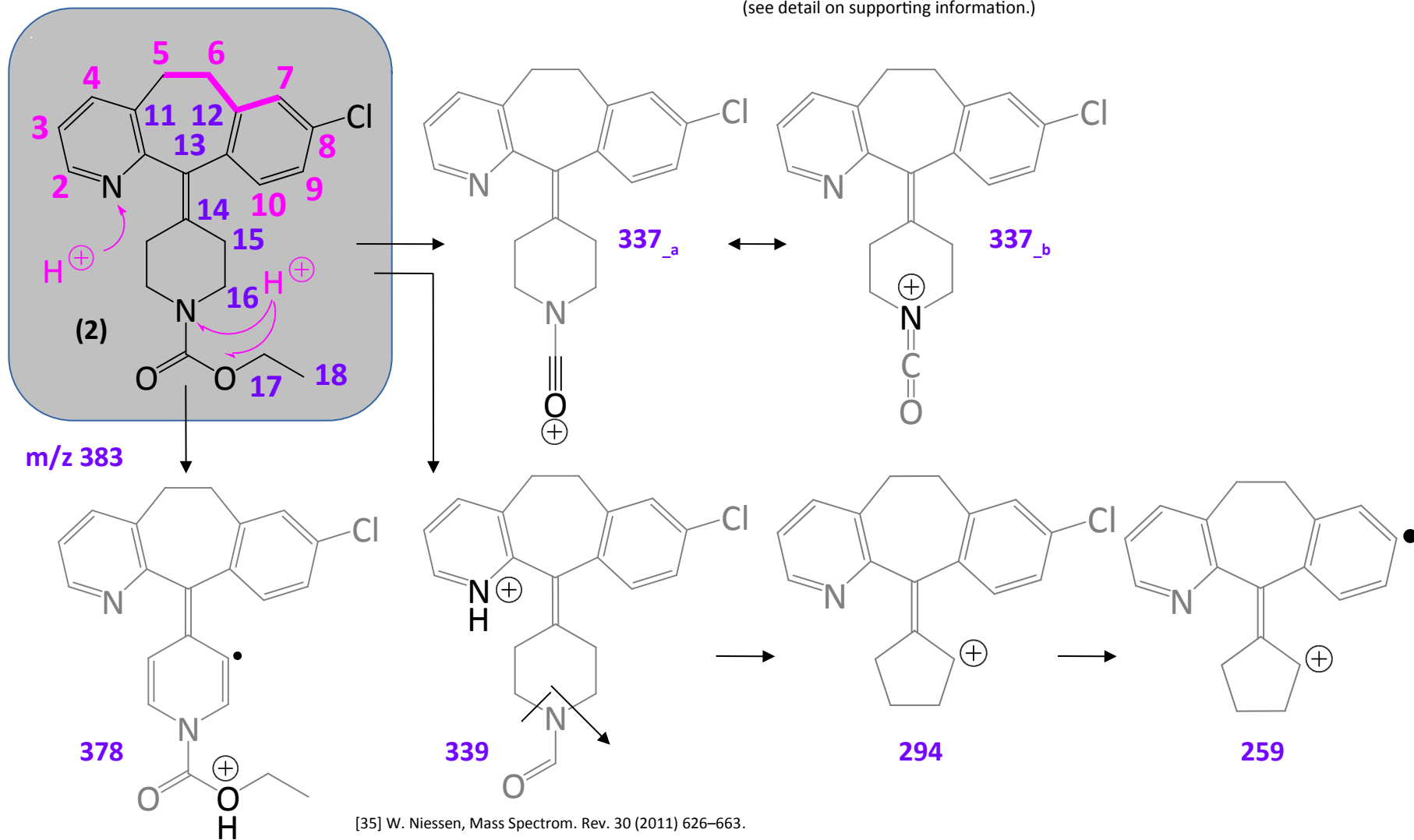


**Figure 3.** Chemical diagrams of diclofenac (1) and its fragmentation MS products [33,34]

(see detail on [supporting information](#).)

[33] M. Galmier, B. Bouchon, J. Madelmont, F. Mercier, F. Pilotaz, C. Lartigue, J. Pharmaceut. Biomed. Anal. 38 (2005) 790–796.

[34] S. Perez, D. Barcelo, Anal. Chem. 80 (2008) 8135–8145.



[35] W. Niessen, *Mass Spectrom. Rev.* 30 (2011) 626–663.

[36] R. Ramanathan, A. Su, N. Alvarez, N. Blumenkrantz, S. Chowdhury, K. Alton, J. Patrick, *Anal. Chem.* 72 (2000) 1352–1359.



For the purpose of this study, as the title highlights, there are examined quantitatively isotope shapes of molecular and fragment ions of analytes (1) and (2). In this context, the so-called *monoisotopic* MS peak (MP), denotes observable peak of charged molecular ion  $[M]^+$  or protonated cation  $[M+H]^+$  of analyte consisting of only main isotopes of atoms such as, for example,  $^{12}\text{C}$ -,  $^1\text{H}$ -,  $^{14}\text{N}$ -,  $^{35}\text{Cl}$ -,  $^{16}\text{O}$ -, *et cetera* [37–40]. There are observed isotopic clusters of peaks next to MP of the analyte in a difference in  $m/z$  values  $\Delta(m/z)=1$ . The first of them,  $[MP+1]$  contains main isotopes and only one isotope of  $^{13}\text{C}$ -atom. The isotope cluster  $[MP+2]$ , contains two  $^{13}\text{C}$ -atoms or one  $^{13}\text{C}$ - and one  $^{15}\text{N}$ -atom, for example (**Figure 5**.) Those, observable multiple-peak systems of isotope clusters can be very complex: thus, remaining hidden fine structures of each of the cluster MS peaks. Despite, employment in ultra-high MS resolving power allows us to resolve fine structure of discussed peaks of isotope shape of cationic species of analyte. Generally, in cases of organics the cluster peaks  $[MP+n]$  ( $n = 1, 2, 3, \dots$ ) refer to  $^{13}\text{C}$ -peaks (**Figure 6**.)

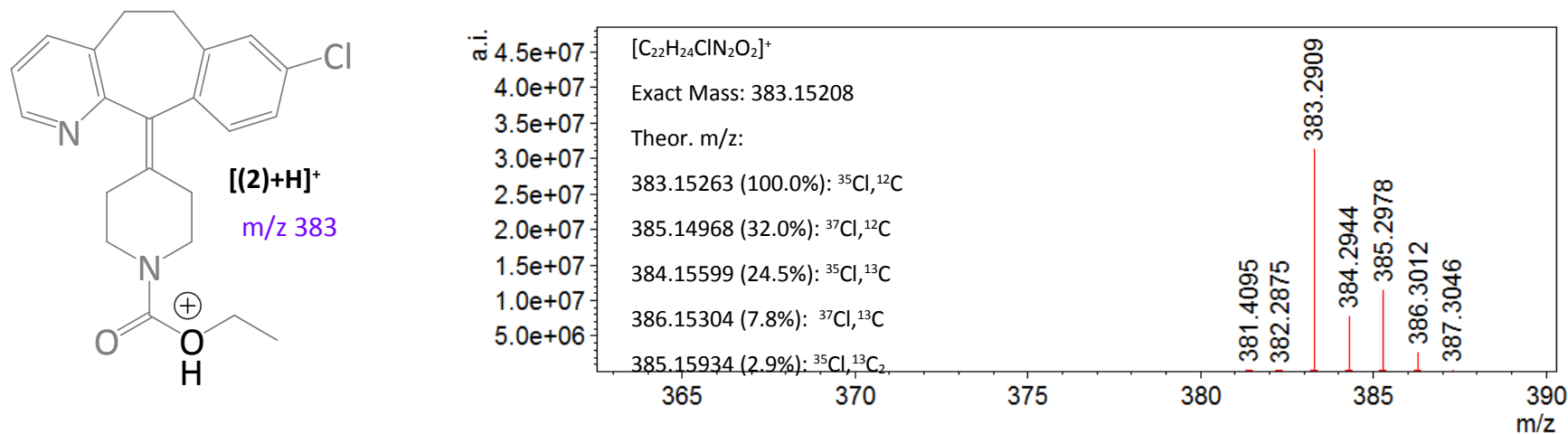


**Figure 5.** Experimental ESI-MS spectrum of loratadine (2), showing isotope shape at  $m/z$  383 of  $[M+H]^+$  cation; theoretical exact mass,  $m/z$  values, and intensity ratios (%) of MS peaks of the isotope shape; chemical diagram of protonated cationic form of (2).

[37] E. Nikolaev, R. Jertz, A. Grigoryev, G. Baykut, *Anal. Chem.* 84 (2012) 2275–2283.

[38] K. Nagornov, M. Gorshkov, A. Kozhinov, Y. Tsybin, *Anal. Chem.* 86 (2014) 9020–9028.

[39] H. Budzikiewicz, R. Grigsby, *Mass Spec. Rev.* 25 (2006) 146–157.

[40] J. Claesen, A. Rockwood, M. Gorshkov, D. Valkenborg, *Mass Spec. Rev.* (2023) 1–21.

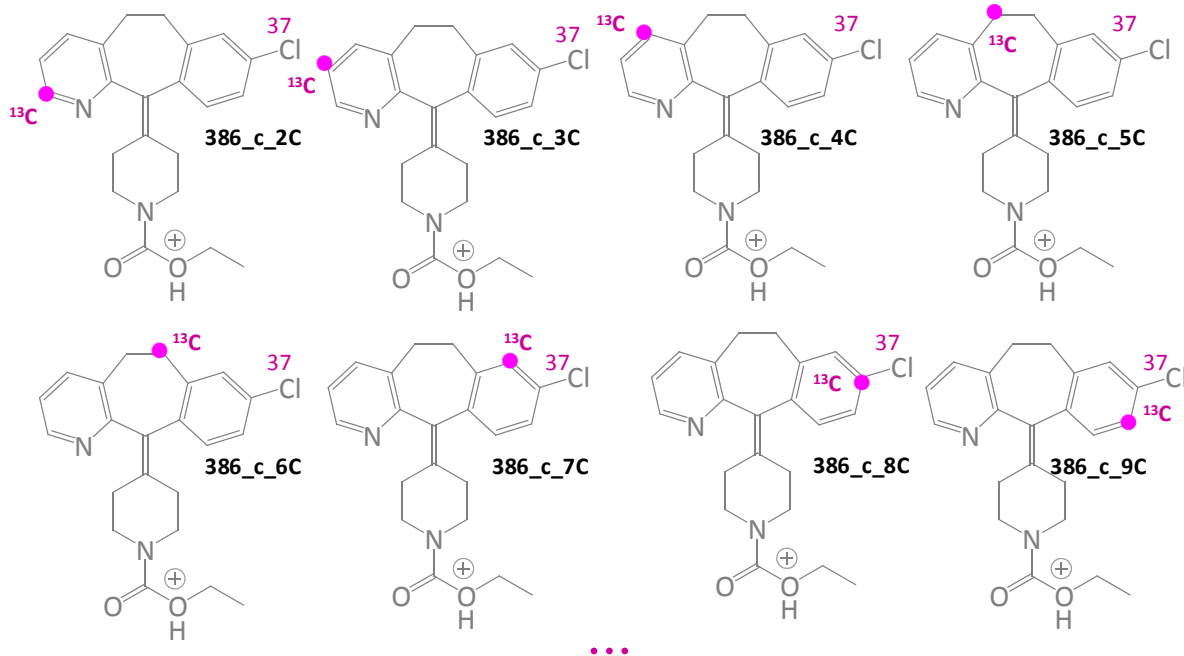


**Figure 6.**  $^{13}\text{C}$ -isotope specific positions of loratadine (2) examining the MS peak  $m/z$  386 of  $[\text{M}+\text{H}]^+$  cation of the analyte (see **Figure 2**);

Molecular isotopologies provide relative isotopic abundance of analytes. It increases in reliability of data on analyte identification and annotation, which is of particular importance for purposes of routine implementation of omics-protocols into *clinical precision medicine*, because of high standard chemometric method performances of omics-analyses are compulsory. However, *fluctuations* in elemental composition are caused by isotope fractionation determined by (bio)chemical and geochemical processes [40]. They induce differences in isotope ratio among isotopes of the same atom: thus causing for errors in *proteomics* [41] or *isotomics* [40]. Highly precise MS measurements of molecular isotopologies contribute crucially not only to the field of medicine and clinical diagnostics, but also to ecology, geology or history, in addition to *forensic anthropology*, where so-called *isoscapes* from human body tissues such as teeth, nails, bone and hair, allow to predict region-of-origin of human remains [42]. Due to, these reasons, fractional labelling of analytes must be obtained accurately. Accurate measurands of *fractional abundance* of molecular isotopologies of analyte refers to so-called *spectral accuracy* [43].

[41] J. Claesen, F. Lermyte, F. Sobott, T. Burzykowski, D. Valkenburg, *Anal. Chem.* 87 (2015) 10747–10754

[42] E. Bartelink, L. Chesson, *Forensic Sci. Res.* 4 (2019) 29–44.

[43] X. Su, W. Lu, J. Rabinowitz, *Anal. Chem.* 89 (2017) 5940–5948



# The 9th International Electronic Conference on Medicinal Chemistry

01–30 November 2023 | Online



CE = 10 V								
C <sub>FA</sub> =0.2M								
Scan	m/z	I [arb.units]	m/z	I [arb.units]	m/z	I [arb.units]	m/z	I [arb.units]
01	296.11807	2.13.10 <sup>6</sup>	297.24692	291324.328	298.12494	1.29.10 <sup>6</sup>	301.38605	107508.059
02	296.11807	2.27.10 <sup>6</sup>	297.12149	375839.217	298.12494	1.35.10 <sup>6</sup>	301.26062	122320.882
03	296.11807	2.09.10 <sup>6</sup>	297.24692	331929.321	298.12494	1.27.10 <sup>6</sup>	301.13522	98668.778
04	296.11807	2.16.10 <sup>6</sup>	297.12149	277727.366	298.12494	1.43.10 <sup>6</sup>	301.26062	98168.7215
05	296.11807	2.09.10 <sup>6</sup>	297.12149	374971.519	298.12494	1.44.10 <sup>6</sup>	301.38605	99537.7983
06	296.11807	2.22.10 <sup>6</sup>	297.12149	305343.558	297.99948	1.28.10 <sup>6</sup>	301.26062	82198.3022
07	295.99265	1.90.10 <sup>6</sup>	297.12149	258503.749	298.12494	1.19.10 <sup>6</sup>	301.26062	119635.458
08	296.11807	1.97.10 <sup>6</sup>	297.12149	349880.275	298.12494	1.19.10 <sup>6</sup>	301.26062	121683.97
09	296.24347	2.04.10 <sup>6</sup>	297.12149	293467.267	298.25037	1.15.10 <sup>6</sup>	301.13522	82016.6479
10	296.11807	2.07.10 <sup>6</sup>	297.12149	386088.469	298.12494	1.38.10 <sup>6</sup>	301.26062	128442.379
11	296.11807	2.04.10 <sup>6</sup>	296.99609	283941.018	298.12494	1.45.10 <sup>6</sup>	301.13522	105097.172
12	296.11807	1.96.10 <sup>6</sup>	297.12149	332191.988	298.12494	1.36.10 <sup>6</sup>	301.26062	99901.9127
Mean	296.11807		297.13195		298.12494		301.25018	
sd(yEr±)	0.05348		0.06458		0.05349		0.08384	
se(yEr±)	0.01544		0.01864		0.01544		0.0242	
<I>		2.07745.10 <sup>6</sup>		321767.33964		1.31493.10 <sup>6</sup>		105431.67333
<I> <sup>2</sup>		4.3157985025.10 <sup>12</sup>		1.03534220859.10 <sup>11</sup>		1.7290409049.10 <sup>12</sup>		1.111583774.10 <sup>10</sup>
<I <sup>2</sup> >		4.32613.10 <sup>12</sup>		1.05223.10 <sup>11</sup>		1.73862.10 <sup>12</sup>		1.13272.10 <sup>10</sup>
<I <sup>2</sup> >-<I> <sup>2</sup>		1.03314975.10 <sup>10</sup>		1.688779140997.10 <sup>9</sup>		9.5790951.10 <sup>9</sup>		2.1136225884.10 <sup>8</sup>
D <sub>SD</sub>		2.7262755603.10 <sup>-7</sup>		4.456350397263.10 <sup>-8</sup>		2.5277316149.10 <sup>-7</sup>		5.5774272862.10 <sup>-8</sup>
CE = 20 V								
C <sub>FA</sub> =0.2M								
Scan	m/z	I [arb.units]	m/z	I [arb.units]	m/z	I [arb.units]	m/z	I [arb.units]
01	295.99265	2.59.10 <sup>6</sup>	297.12149	4.85.10 <sup>5</sup>	298.12494	1.89.10 <sup>6</sup>	301.13522	1.93.10 <sup>5</sup>
02	296.11807	2.86.10 <sup>6</sup>	296.99609	349833.532	298.12494	1.73.10 <sup>6</sup>	301.26062	1.66.10 <sup>5</sup>
03	296.11807	2.92.10 <sup>6</sup>	297.12149	3.63.10 <sup>5</sup>	298.12494	1.85.10 <sup>6</sup>	301.26062	1.82.10 <sup>5</sup>
04	296.11807	2.99.10 <sup>6</sup>	296.99609	360901.115	298.12494	1.78.10 <sup>6</sup>	301.13522	2.26.10 <sup>5</sup>
05	296.11807	2.86.10 <sup>6</sup>	297.12149	378684.441	298.12494	1.79.10 <sup>6</sup>	301.13522	167262.776
06	296.11807	2.96.10 <sup>6</sup>	297.12149	450949.68	298.12494	1.70.10 <sup>6</sup>	301.26062	221801.268
07	296.11807	2.33.10 <sup>6</sup>	297.12149	342321.674	298.12494	1.81.10 <sup>6</sup>	301.13522	131386.564
08	296.11807	2.95.10 <sup>6</sup>	297.12149	472503.448	298.12494	2.13.10 <sup>6</sup>	301.13522	182346.207
09	296.11807	3.00.10 <sup>6</sup>	296.99609	504985.083	298.12494	1.88.10 <sup>6</sup>	301.13522	107686.17
10	296.11807	2.91.10 <sup>6</sup>	297.12149	492028.32	298.12494	1.90.10 <sup>6</sup>	301.13522	230684.695
11	296.11807	2.73.10 <sup>6</sup>	297.12149	409902.594	298.12494	2.10.10 <sup>6</sup>	301.13522	153614.439
Mean	296.10667		297.08729		298.12494		301.16942	
sd(yEr±)	0.03782		0.05857		0		0.05857	
se(yEr±)	0.0114		0.01766		0		0.01766	
<I>		2.82853.10 <sup>6</sup>		419090.61195		1.86618.10 <sup>6</sup>		178354.04928
<I> <sup>2</sup>		8.00058196.10 <sup>12</sup>		1.75636941025.10 <sup>11</sup>		3.4826277924.10 <sup>12</sup>		3.18101669.10 <sup>10</sup>
<I <sup>2</sup> >		8.03832.10 <sup>12</sup>		1.79257.10 <sup>11</sup>		3.49978.10 <sup>12</sup>		3.31964.10 <sup>10</sup>
<I <sup>2</sup> >-<I> <sup>2</sup>		3.77380391.10 <sup>10</sup>		3.620058975375.10 <sup>9</sup>		1.71522076.10 <sup>10</sup>		1.386233105.10 <sup>9</sup>
D <sub>SD</sub>		9.95831376.10 <sup>-7</sup>		9.55261162422.10 <sup>-8</sup>		4.52612454.10 <sup>-7</sup>		3.657991918.10 <sup>-8</sup>

Equation (4) it is derived from equation (1) [15]. It connects between  $\langle I \rangle^{\text{TOT}}_{\text{Theor}}$  values of analyte fragmentation ions measured toward experimental parameters such as collision energy and  $D''_{\text{SD}}$  data on equation (2). The statistical factors  $A_D^q$  and  $A_I^q$  are *functional amplitudes* of SineSqr function. It is fitted of relations  $D''_{\text{SD}} = f(\text{CE})$  and  $\langle I \rangle^q = f(\text{CE})$  of  $q^{\text{th}}$  MS analyte fragmentation ion. Looking at new empirical proof of equation (4), let us detail on measurands of analytes (1) and (2) (**Table 1**). Relations  $\langle I \rangle^q = f(\text{CE})$  and  $\langle I \rangle^q = f(C_{\text{FA}})$  of ions of (1) and (2) reveal nonlinear relationship showing  $|r| = 0.9769-0.49583$  (1). Loratadine (2) exhibits  $\langle I \rangle^q = f(\text{CE})$  function, showing  $|r| = 0.99962-0.95594$  (**Figures 7 and 8**). Generally, there is inapplicability of linear model to fit quantitatively  $\langle I \rangle^q = f(\text{CE})$  and  $\langle I \rangle^q = f(C_{\text{FA}})$  relations.

**Table 1**

Mass spectrometric measurands such as m/z and intensity values [arb.units] per scan number of diclofenac (1) with respect to concentration of formic acid  $C_{\text{FA}} = 0.2$  M, and collision energy CE=10 and 20 V; descriptive statistics; data on equation (2)

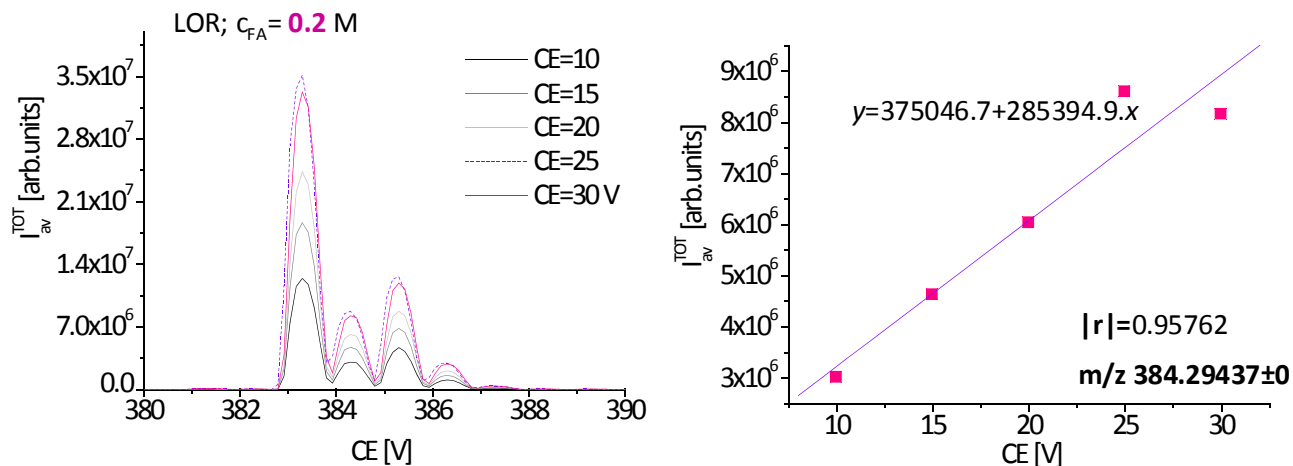


**Figure 7.** Relationships between average total intensity [arb.units] with respect to collision energy (CE=10–30V) of ESI(+)-MS spectrometric variables at concentration of HCOOH ( $C_{FA}=0.2$  M) and within spectrometric range  $m/z=370$ –410; analyte (LOR) concentration 10 pmol; chemometrics.

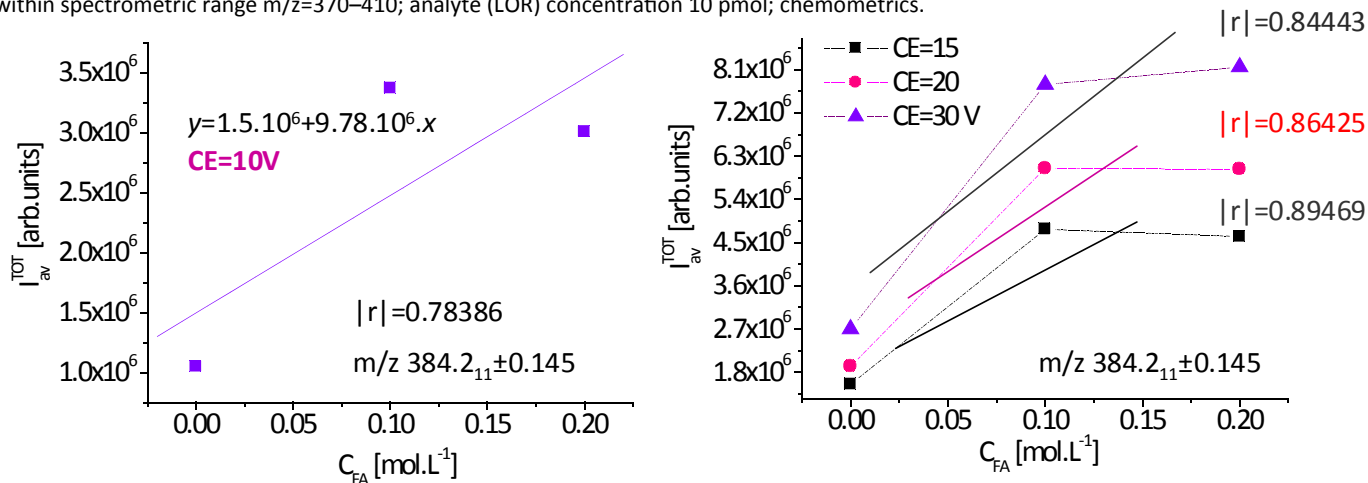


**Figure 8.** Relationships between average total intensity [arb.units] of ions at  $m/z$  383 and 384 of the isotope shape of analyte loratadine with respect to collision energy (CE=10–30V) of ESI(+)-MS spectrometric variables at concentrations of HCOOH ( $C_{FA}=0$ –0.2 mol.L<sup>-1</sup>) and within spectrometric range  $m/z=370$ –410; analyte concentration 10 pmol; descriptive statistics; chemometrics.



**Table 2**

ANOVA data on m/z 296 and 301 of diclofenac (1) with respect to concentration of formic acid  $C_{FA} = 0.2$  M, and collision energy  $CE=10-30$  V

Dataset	N	Mean	sd(yEr±)	se(yEr±)	
Data61_A	6	301.26062	0		
Data61_B	6	301.19794	0.15362	0.06271	
H <sub>0</sub> : The means of all selected datasets are equal					
H <sub>1</sub> : The means of one or more selected datasets are different					
Source	DoF	Sum of Squares	Mean Square	F Value	P Value
Model	1	0.0117875150	0.0117875150	0.99903	0.34112
Error	10	0.117989955	0.0117989955		
At the 0.01 level, the population means are not significantly different.					
Means Comparison using Bonferroni Test					
Dataset	Mean	Difference between means	Simultaneous Confidence Intervals		Significant at 0.01 Level
Data64_20	301.26062		Upper Limit	Lower Limit	
Data64_25	301.19794	0.06268	-0.13607	0.26144	No
Dataset	N	Mean	sd(yEr±)	se(yEr±)	
	4	296.99609	0		
	7	297.12149	5.11323.10 <sup>-6</sup>	1.93262.10 <sup>-6</sup>	
H <sub>0</sub> : The means of all selected datasets are equal					
H <sub>1</sub> : The means of one or more selected datasets are different					
Source	DoF	Sum of Squares	Mean Square	F Value	P Value
Model	1	0.0400236805	0.0400236805	2.29624E9	0
Error	9	1.56870629.10 <sup>-10</sup>	1.74300699.10 <sup>-11</sup>		
At the 0.01 level, the population means are not significantly different.					
Means Comparison using Bonferroni Test					
Dataset	Mean	Difference between means	Simultaneous Confidence Intervals		Significant at 0.01 Level
Data64_20	296.99609		Upper Limit	Lower Limit	
Data64_25	297.12149	-0.12539	-0.1254	-0.12539	Yes

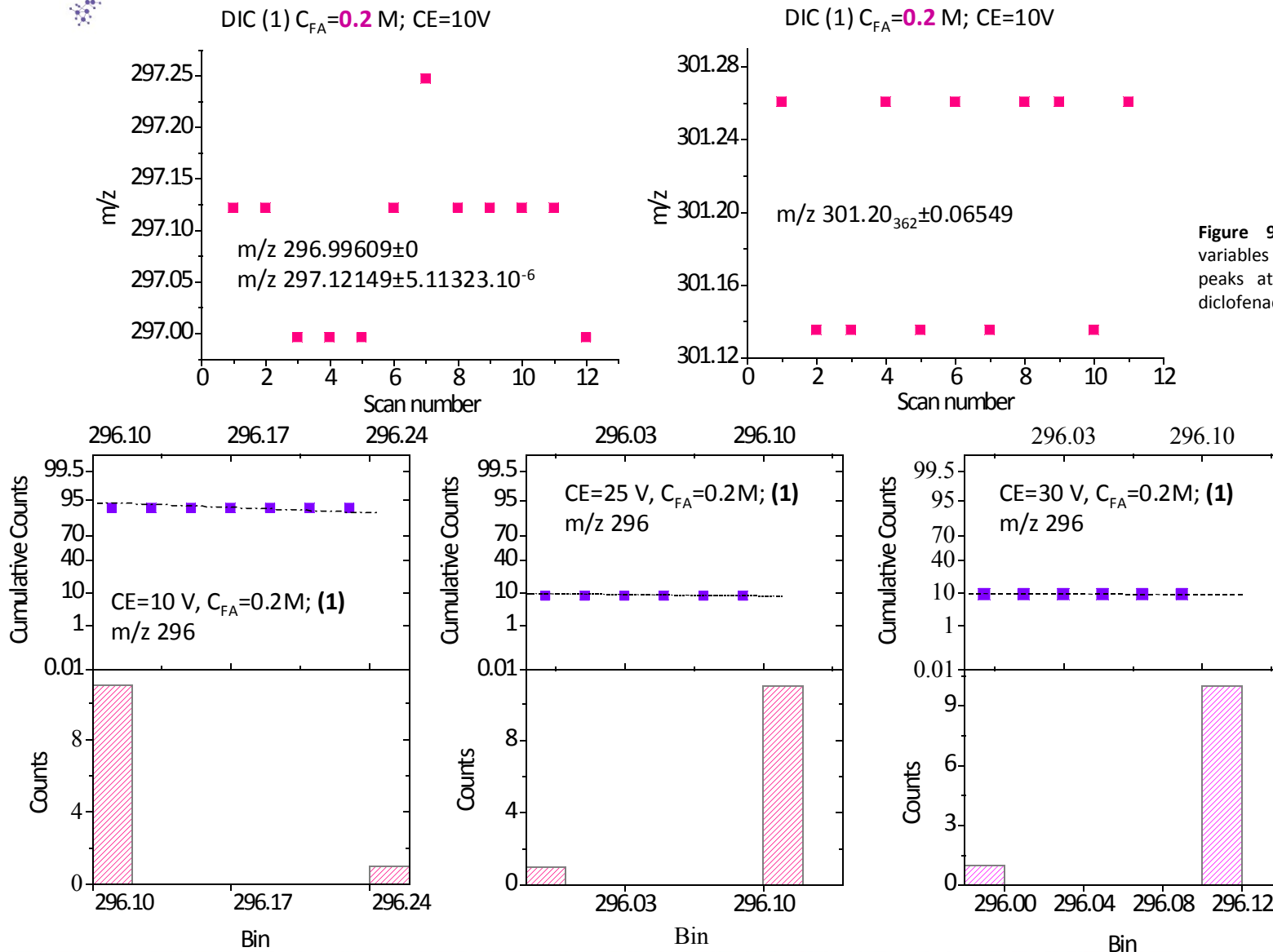
Functional relationships according to equation (4) are determined within the same peaks of isotope shape of analyte cations. Theoretical  $\langle I \rangle_{\text{theor}}$  data on ions with respect to CEs, and  $A_D^q$ ,  $A_I^q$  parameters as listed in **Figures 11** and **12** are correlated with experimental  $\langle I \rangle_{\text{exp}}$  data on (1) (**Figure 13**) There is  $|r|=0.96701$ . The deviation of the coefficient from exact value  $|r|=1$  is, due to error contribution to  $I_{\text{av};\text{exp}}^{\text{TOT}}$  data on intensity of MS ions of different m/z measurands per short span of scan time, which are statistically significantly different (**Figure 9.**) MS peaks at m/z 296.24347 and 295.99265 are different from 296.11807 one, which, however, is mainly observed within the studied spans of scan time of MS spectra of (1) at  $C_{FA}=0.2$  M and  $CE=10$  V.

ANOVA tests are applied to normally distributed variables (**Figure 9.**) Looking at histograms and probability plots (**Figure 10.**) when the plot lies from a line, then random quantities are normally distributed. Conversely, when there is a deviation from linear plot, then variables can be outlier. The histogram and probability plots of m/z-data show a lack of point out of the line. The variables are normally distributed. However, W-statistics show small W-values, thus assuming a not normal distribution. This result could be interpreted as follows. Shapiro-Wilk the test is not robust. it is used to histogram and probability plots of measurands, assuming normal distribution of random variables. Moreover, detail on measurands at m/z 297, 298 and 301 shows a discrete sets of variables, belonging to molecular *isotopologies*. ANOVA data on m/z 301 reveals that variables are not statistically significantly different. Therefore, there is a single peak at m/z 301.20<sub>362</sub> ± 0.06549. Conversely, results from variables at m/z 297 show two sets of variables, which are statistically significantly different (**Table 2.**) There are two sets of values at m/z 296.99609 ± 0 and 297.12149 ± 5.11323.10<sup>-6</sup>. The data on latter table clearly underline that without employment in ANOVA test on distinguishing statistically variables, there is unable to assign correctly isotope MS peaks of an isotope shape.



# The 9th International Electronic Conference on Medicinal Chemistry

01–30 November 2023 | Online



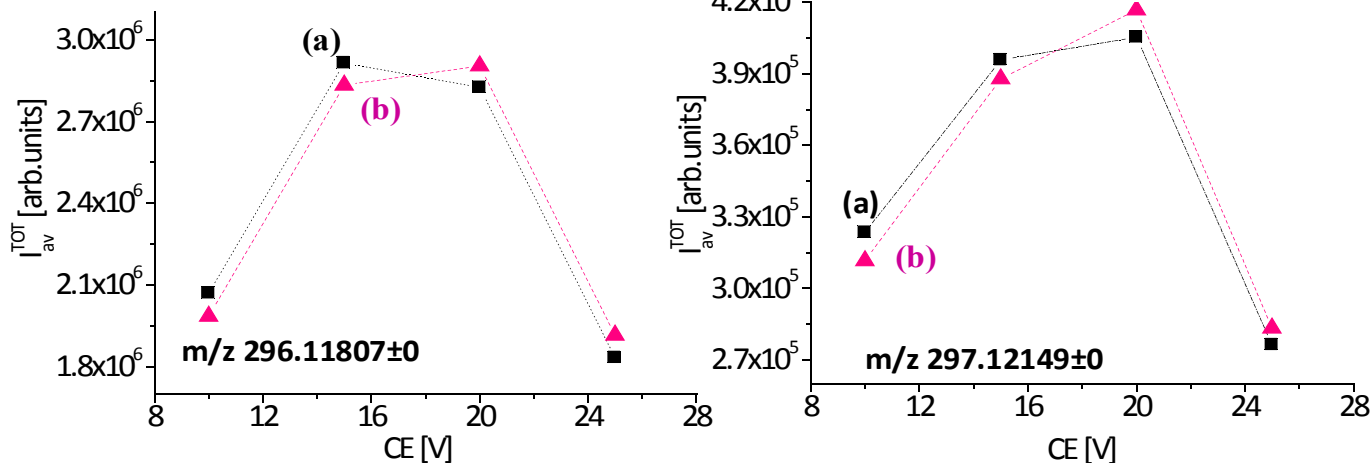


# The 9th International Electronic Conference on Medicinal Chemistry

01–30 November 2023 | Online

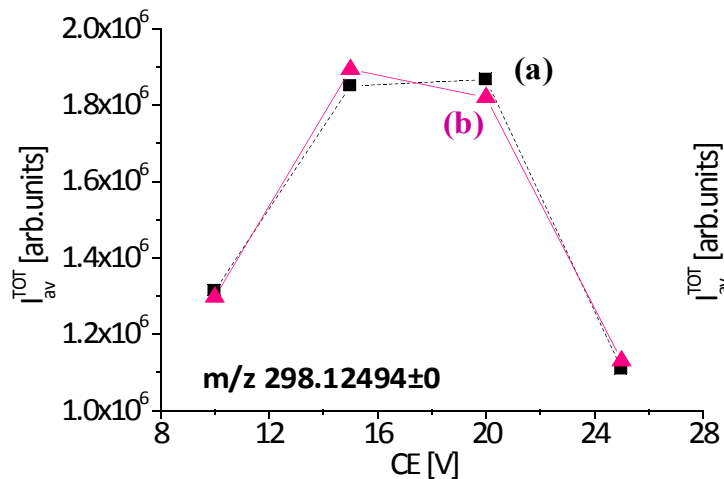


DIC (1)  $C_{FA}=0.2$  M

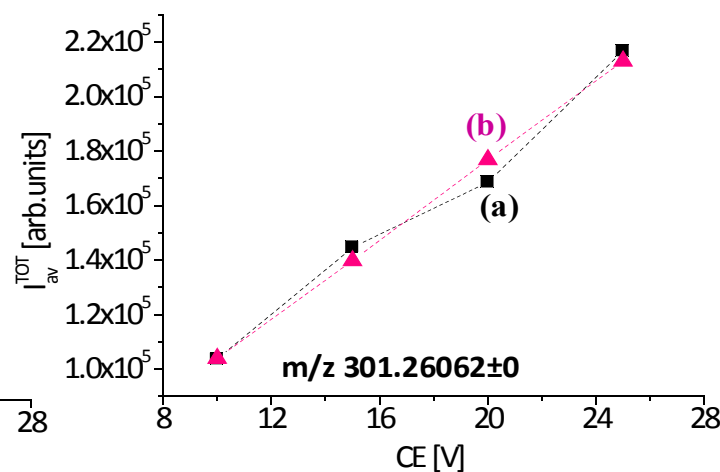


$A_q=5275295.07\pm181169.39$

$A_q=751872.49\pm21595.9$



$A_q=1954348.64\pm47922.44$



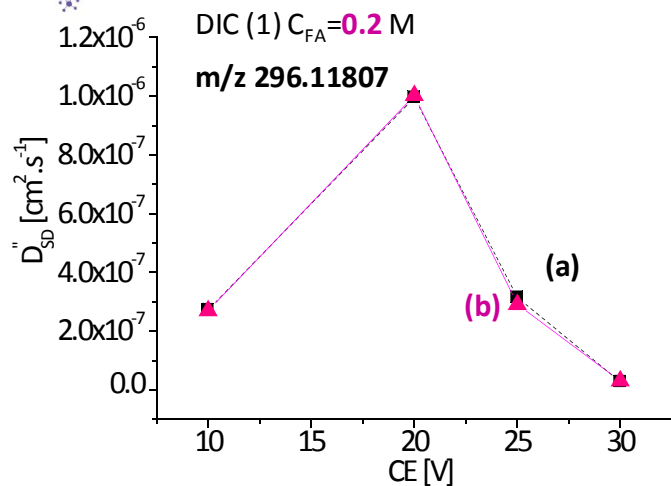
$A_q=323965.94\pm85563.17$

**Figure 11.** Relationships between average total intensity [arb.units] with respect to collision energy (CE=10–25V) of ESI(+)-MS spectrometric variables of MS ions at concentration of HCOOH ( $C_{FA}=0.2$  M) and within spectrometric range  $m/z=200-300$ ; analyte diclofenac (DIC) concentration 15 pmol (a); SineSqr approximation of the latter relationship (b); chemometrics.

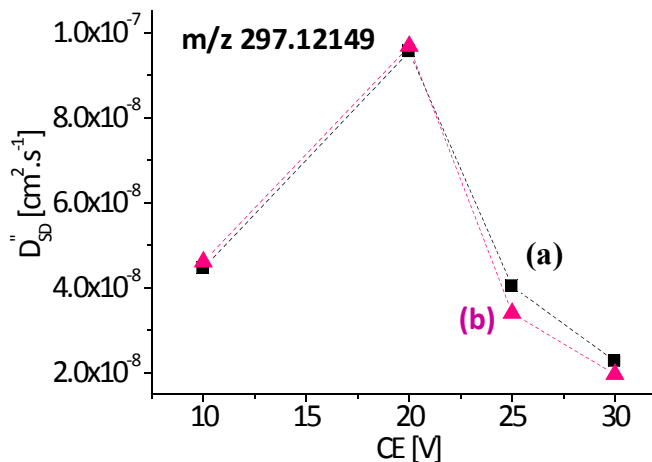


# The 9th International Electronic Conference on Medicinal Chemistry

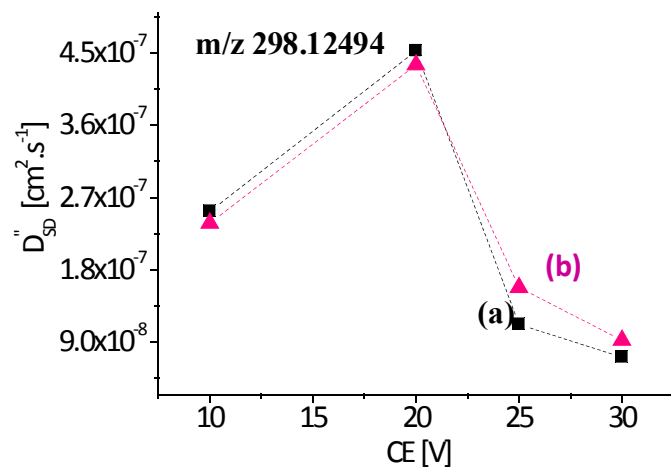
01–30 November 2023 | Online



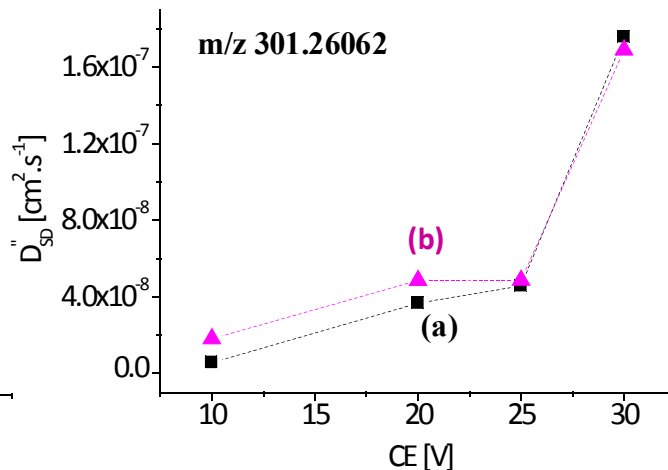
$$A^q_D = 1.1262 \cdot 10^{-6} \pm 3.213 \cdot 10^{-8}$$



$$A^q_D = 9.8877 \cdot 10^{-8} \pm 7 \cdot 10^{-9}$$



$$A^q_D = 4.4832 \cdot 10^{-7} \pm 5.47 \cdot 10^{-8}$$

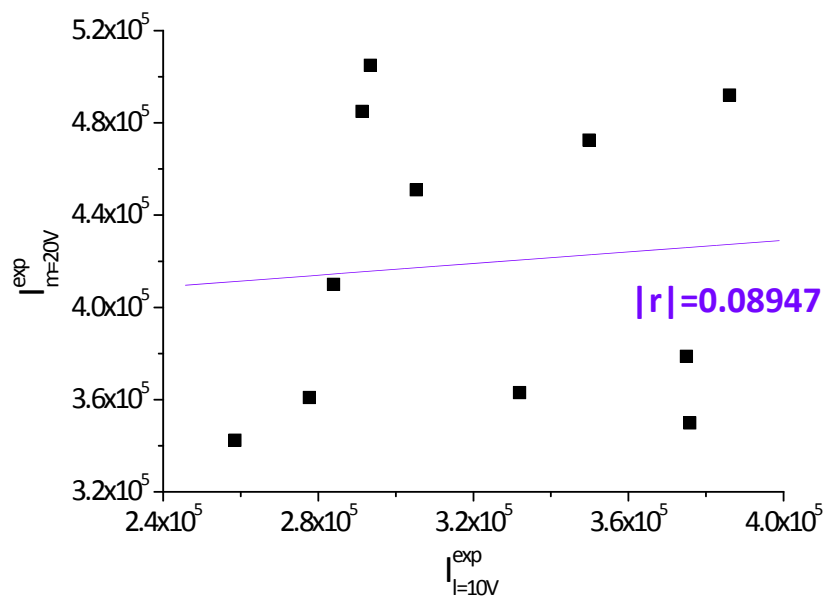


$$A^q_D = 1.7121 \cdot 10^{-7} \pm 1.88 \cdot 10^{-8}$$

**Figure 12.** Relationships between  $D''_{SD}$  [ $\text{cm}^2 \cdot \text{s}^{-1}$ ] parameters of equation (2) with respect to collision energy (CE=10–25V) of ESI(+)-MS spectrometric variables of MS ions at concentration of HCOOH ( $C_{FA}=0.2$  M) and within spectrometric range  $m/z=200$ – $300$ ; analyte diclofenac (DIC) concentration 15 pmol (a); SineSqr approximation of the latter relationship (b); chemometrics.



**NB!**



## How is obtained $|r_{l,m}|$ value?

It is linear correlation coefficient of relationship between experimental total intensity data determined *per* short span of scan time of two sets of MS measurement conditions (l and m.)

For instance, consider data on l=10 and m=20 V (Table 1.)

$$D''_{SD,l} + D''_{SD,m} = |r_{l,m}| \times \sqrt{I_{l,q}^2 - (\overline{I_{l,q}})^2} \times \sqrt{I_{m,q}^2 - (\overline{I_{m,q}})^2}$$

Equation (5)

**NB!**

The contribution uses term *fragmentation ion* instead of *fragment ion*; thus, following IUPAC standards: K. Murray, R. Boyd, M. Eberlin, G. Langley, L. Li, Y. Naito, Definitions of terms relating to mass spectrometry (IUPAC Recommendations 2013). Pure Applied Chemistry. 85 (2013) 1515–1609.



# The 9th International Electronic Conference on Medicinal Chemistry

01–30 November 2023 | Online

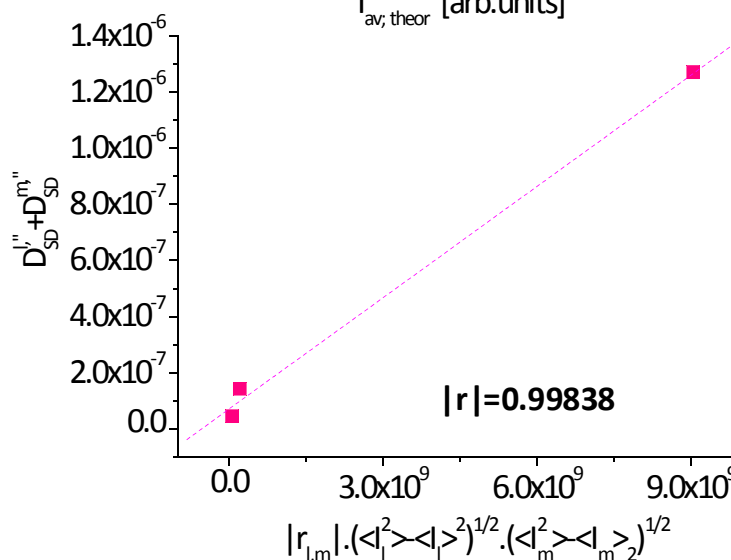
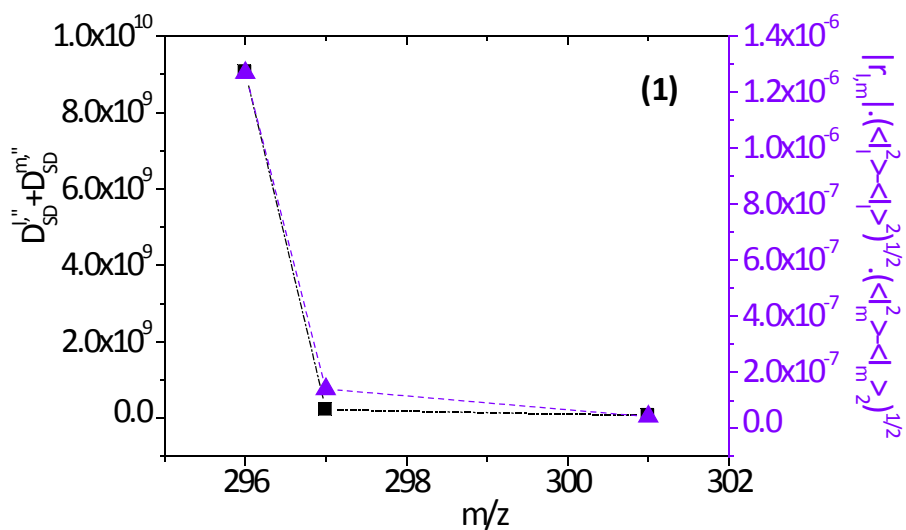
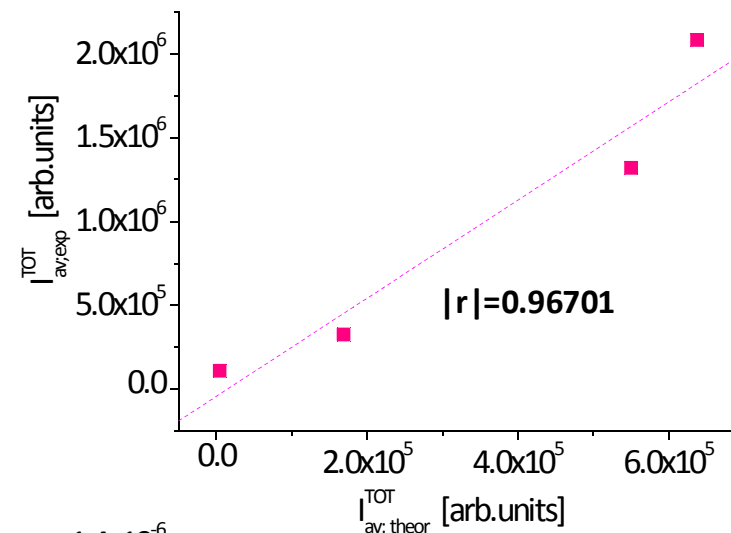
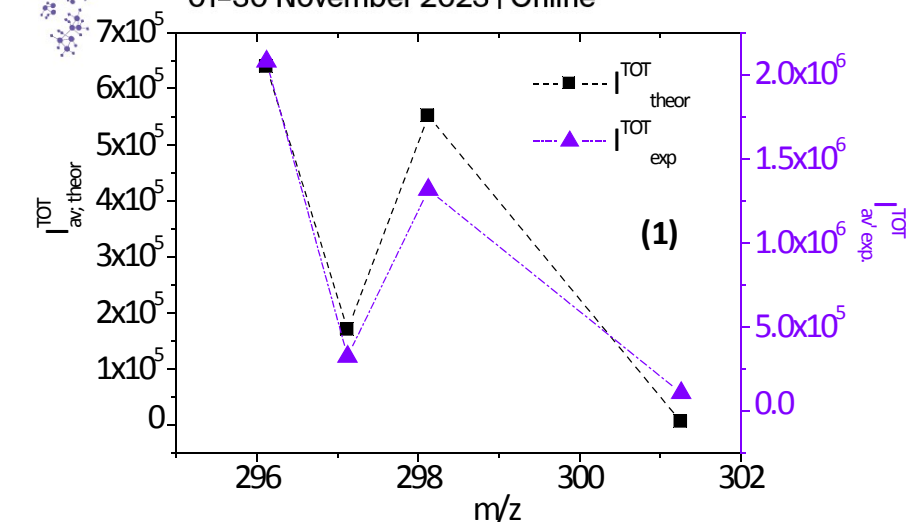


**Figure 13.** Relationships between theoretical and experimental average total intensity [arb.units] data on analyte (1) with respect to collision energy (CE=10–25V) of ESI(+)-MS spectrometric variables of MS ions at concentration of HCOOH ( $C_{FA}=0.2$  M) according to **equation (4)** (A); correlation between parameters according to **equation (5)** of the same analyte with respect to collision energy  $l=10$  and  $m=20$  V; the  $|r_{l,m}|$  parameters are 0.45902 (m/z 296), 0.08947 (m/z 297), and 0.12502 (m/z 301) (B); chemometrics.



## 2. Theoretical quantum chemical data

For our purposes important computational quantum chemical method, amongst others, is that of determining molecular vibrations by means of **harmonic approximation of Born-Oppenheimer potential energy surface** [41–44]. It exhibits great success in description of molecular properties such as specific heat capacity, thermal expansion, entropy, electronic structure of stationary points, trajectories, reaction dynamics, thermochemistry of GS and TS (**Figure 14,**) molecular kinetics, spectroscopic quantities, *et cetera*, due to the fact that method employs *statistical thermodynamics*. It bridges between microscopic atomic level description of molecular dynamics or quantum-mechanical vibrational both GS and TS of molecules and macroscopic (thermal) properties. The study uses DFT-BOMD computations (**Figure 15**). DFT (**Figure 16**) and MP2 methods with modest basis set are generally recommendable as providing accurate theoretical parameters balancing between accuracy and computational costs [45–47]. As work [47] comprehensively illustrates B3LYP-D3 method, for instance, computing relative and reaction energy values of solvate coordination compounds of transition metal ions, provides accurate energetics comparing with experiment.

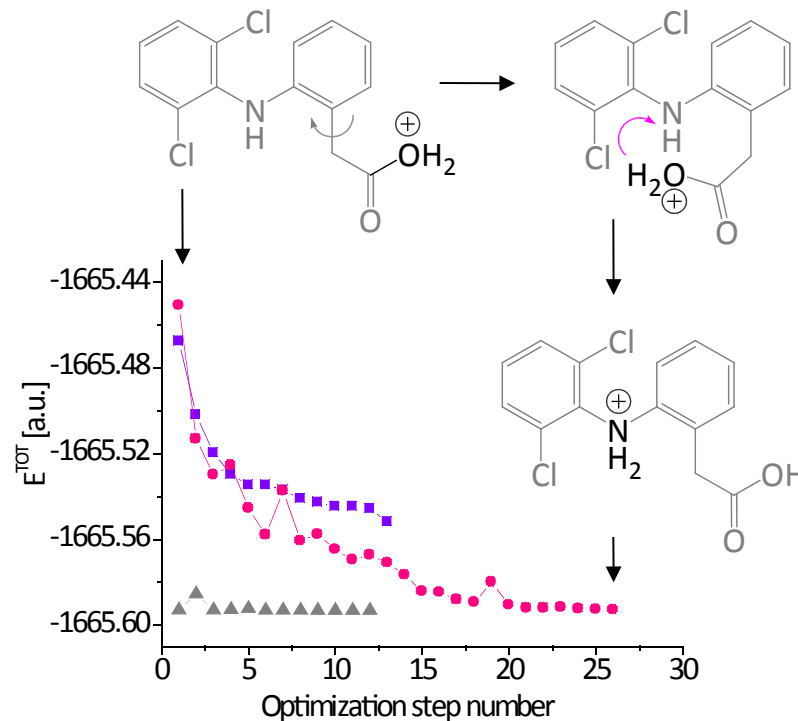


**Figure 14.** DFT (M062X) optimization of protonated  $[M+H]^+$  cation of analyte (1) showing intramolecular proton transfer: Total energy ( $E^{\text{TOT}}$ ) [a.u.] with respect to optimization step number.

[41] A. Erba, J. Maul, M. Ferrabone, P. Carbonnière, M. Rérat, R. Dovesi, J. Chem. Theory Comput. 15 (2019) 3755–3765.

[42] A. Maradudin, E. Montroull, G. Weiss, Theory of lattice dynamics in the harmonic approximation; Academic Press: New York and London (1963) Suppl. 3: Solid state physics, pp. 1–319.

[43] A. Turney, B. Zhang, D. Smith, D. Altarawy, H. Schaefer, III, J. Chem. Theory Comput. 15 (2019) 4386–4398.

[44] R. Conte, C. Aieta, G. Botti, M. Cazzaniga, M. Gandolfi, C. Lanzi, G. Mandelli, D. Moscato, M. Ceotto, Theor. Chem. Accts 143 (2023) 53.

[45] T. Gyori, G. Czako, J. Chem. Theory Comput. 16 (2020) 51–66.

[46] D. Villablanca, S. Gazzari, B. Herrera, Theor. Chem. Accts 142 (2023) 32.

[47] Y. Kumar, N. Kumar, G. Sastry, Theor. Chem. Accts 142 (2023) 35.

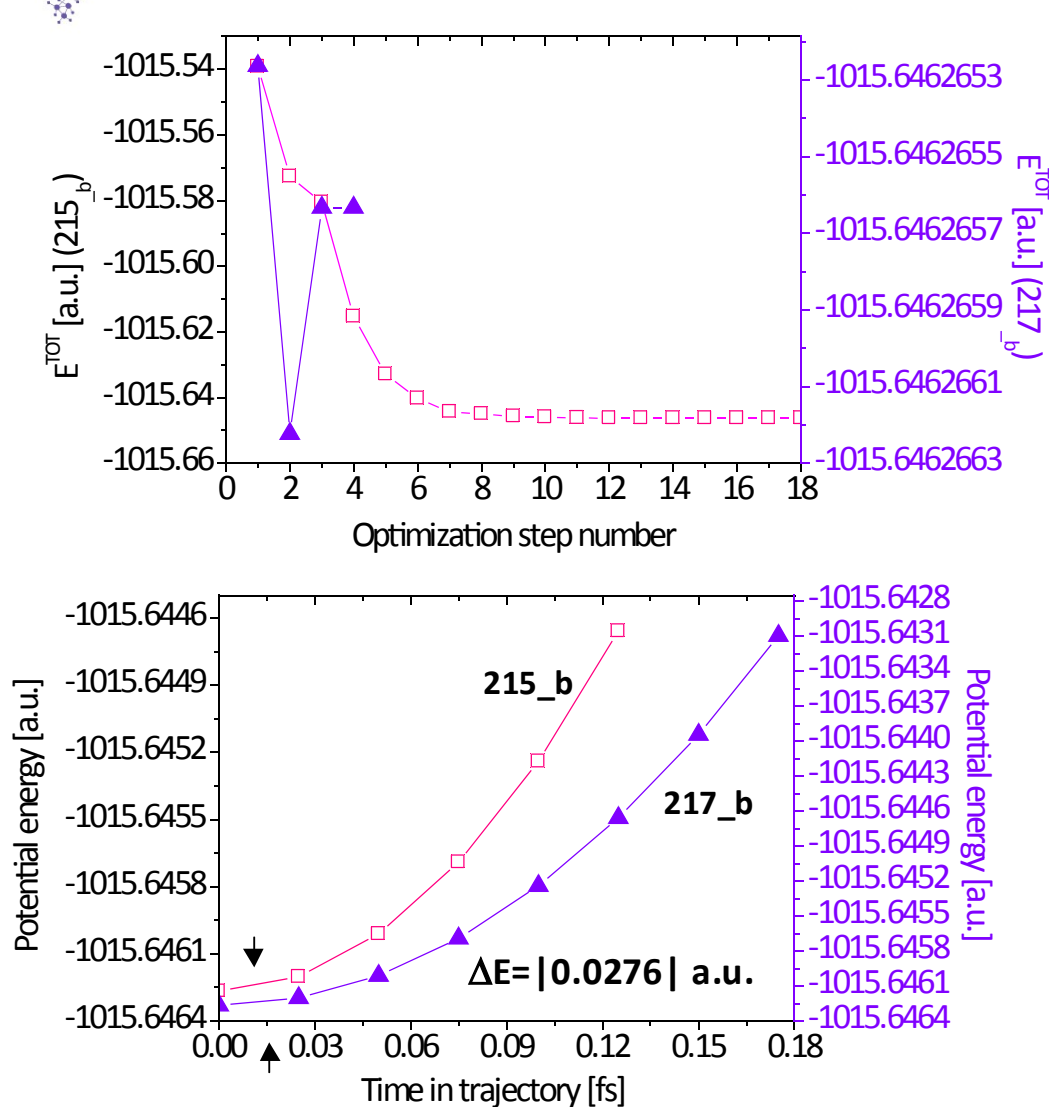


**Figure 15.** DFT (M062X) optimization of fragmentation cation of analyte (1) at m/z 215 and 217: Total energy ( $E^{\text{TOT}}$ ) [a.u.] with respect to optimization step number; BO-molecular dynamics data: Potential energy [a.u.] versus time in trajectory [fs]; difference in energy data ( $\Delta E$ .)

The frequency analysis of species in their ground and transition states is used to compute  $D_{\text{QC}}$  data on equation (3) (Table 3.)



# The 9th International Electronic Conference on Medicinal Chemistry

01-30 November 2023 | Online

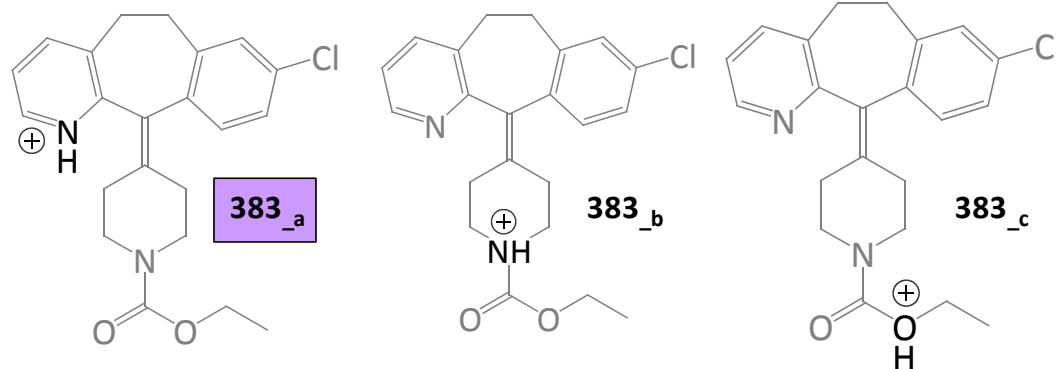
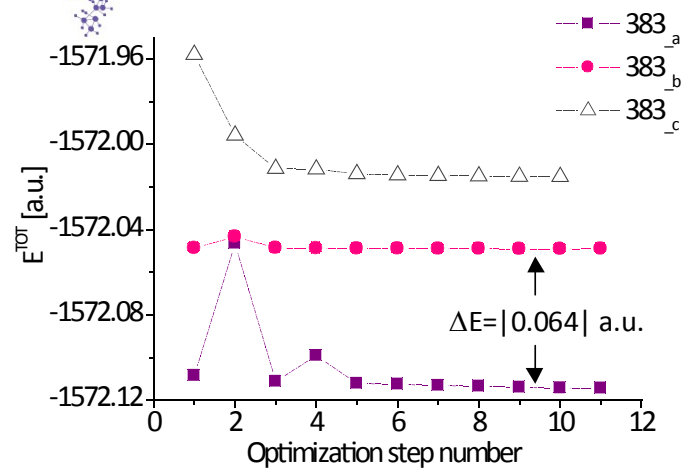
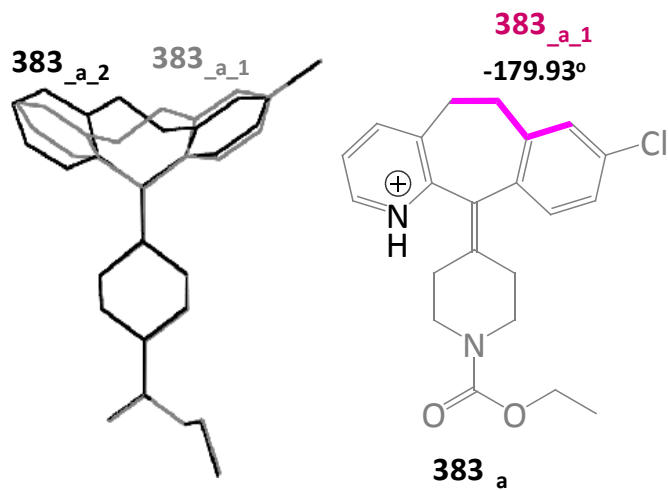


**Figure 16.** DFT (M062X) optimization of  $[M+H]^+$  cation of analyte (2) depending on position of proton: Total energy ( $E^{TOT}$ ) [a.u.] with respect to optimization step number; chemical diagrams of species; most stable 3D molecular conformation depending on the  $C^5-C^6-C-C^7$  dihedral angle value (**Figure 5**.)



Most stable 3D molecular geometry is ion  $383_{a_1}$ , showing protonation at N<sup>1</sup>-position of the molecule of analyte (2) and having  $C^5-C^6-C-C^7$  dihedral angle value  $\angle -179.93^\circ$



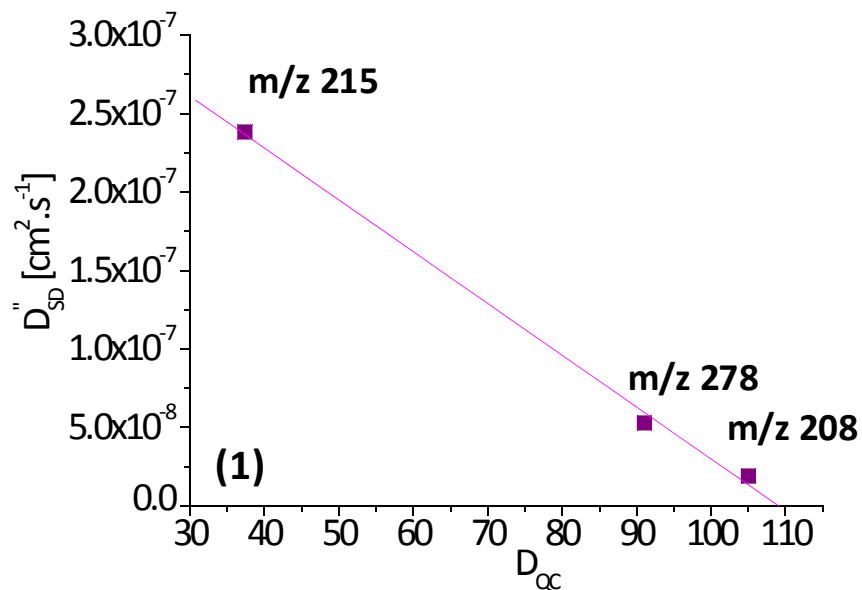
### 3. Correlative analysis between experiment and theory

Following general calculation tasks and *chemometrics* of  $D''_{SD}$  parameters of equation (2) of pharmaceuticals we must begin, with the fact that there are a set of MS measurands of diclofenac (1). The ANOVA tests of variables show statistically significantly different  $m/z$  pairs of values at  $m/z$  208.067161±0/208.19302±0; 215.09839±0/215.217±0; 250.08592±0/250.21136±0; 278.18182±1.52277.10<sup>-6</sup>/278.0564±0; 296.11807±7.94.10<sup>-7</sup>/296.2434±0; and 298.12494±3.273.10<sup>-7</sup>/298.25037±0, respectively. The ratio of abundance of  $m/z$  data on by pairs varies within 8:3–10:2. The results, agree well with reported studies, so far, examining tautomers of analyte fragmentation ions [13,14]; thus, showing the same pairs of discrete  $m/z$  variables, which have been assigned quantitatively to tautomers, again, correlating between  $D''_{SD}$  and  $D_{QC}$  parameters of equations (2) and (3) (**Table 3**). There have been obtained excellent-to-exact  $|r|$ -parameters. Conversely, ANOVA tests of variables of  $m/z$  280.06323 and 280.18869 of (1) indicate that they are not statistically significantly different (**supporting information**). Therefore, there is a value  $m/z$  280.0946±0.05674, belonging to only one 3D molecular and electronic structure of fragmentation ion. Owing to the fact that in the case of diclofenac, the ratio of those different electronic structures or molecular conformations of both of these is chiefly at about 80–62.5 % correlative analysis presented, herein, does not account for presence of small amount of second form of fragmentation ions. Therefore, **Figure 17** has to be understood in the following manner. Due to, aforementioned reasons, there should be a deviation of absolute  $|r|$  =1 value, which has been obtained, examining tautomers of metronidazole, where quantification of measurands has been carried out *per* tautomeric form [14]. Despite, this fact, results from **Figure 17** show  $|r|=0.99862$ , examining MS ions of diclofenac (1).

Diclofenac (1)					
$m/z$	Form	$D_{QC}$	$m/z$	Form	$D_{QC}$
296	296 <sup>(1)</sup> <sub>b</sub>	140.7023	277	277 <sup>(1)</sup>	419.6155 <sub>78</sub>
278	278 <sup>(1)</sup> <sub>a</sub>	91.1693	250	250 <sup>(1)</sup> <sub>a</sub>	105.6881 <sub>8</sub>
	278 <sup>(1)</sup> <sub>b</sub>	55.5705 <sub>5</sub>		250 <sup>(1)</sup> <sub>b</sub>	202.9523 <sub>58</sub>
	278 <sup>(1)</sup> <sub>c</sub>	53.5619 <sub>01</sub>		248	248 <sup>(1)</sup>
215	215 <sup>(1)</sup> <sub>a</sub>	37.4958 <sub>28</sub>	243	243 <sup>(1)</sup>	146.6788 <sub>3</sub>
	215 <sup>(1)</sup> <sub>b</sub>	75.8947 <sub>9</sub>		208	208 <sup>(1)</sup>
217	217 <sub>b</sub>	38.42796	178	178 <sup>(1)</sup>	109.2804 <sub>1</sub>
Loratadine (2)					
$m/z$	Form	$D_{QC}$	$m/z$	Form	$D_{QC}$
383	383 <sup>(2)</sup> <sub>c 1a</sub>	66.4553 <sub>5</sub>	384	384 <sup>(2)</sup> <sub>a 1a C4</sub>	83.84224
	383 <sup>(2)</sup> <sub>a 1a</sub>	89.4761 <sub>5</sub>		248	248 <sup>(2)</sup> <sub>a</sub>
384	384 <sup>(2)</sup> <sub>a 1a C2</sub>	89.9996 <sub>1</sub>	337	248 <sup>(2)</sup> <sub>b</sub>	38.2864
	384 <sup>(2)</sup> <sub>a 1a C3</sub>	83.3262 <sub>5</sub>		337 <sup>(2)</sup> <sub>a</sub>	119.6811 <sub>3</sub>
385	385 <sup>(2)</sup> <sub>c 1a</sub>	124.2983 <sub>5</sub>	337 <sup>(2)</sup> <sub>b</sub>	150.8789	
259	259 <sup>(2)</sup> <sub>a</sub>	39.3346 <sub>8</sub>			
	259 <sup>(2)</sup> <sub>b</sub>	2428.6197			

**Table 3**

$D_{QC}$  data on equation (3) of fragmentation ions of analytes (1) and (2)



Parameter	Value	Error	
A	$3.60095 \cdot 10^{-7}$	$1.4456 \cdot 10^{-8}$	
B	$-3.30201 \cdot 10^{-9}$	$1.74 \cdot 10^{-10}$	
$ r $	$sd(yEr\pm)$	N	$p$
<b>0.99862</b>	$8.77386 \cdot 10^{-9}$	3	0.03346

**Figure 17.** Correlative analysis between  $D''_{SD}$  and  $D_{QC}$  data on equations (2) and (3) of MS fragmentation ions of analyte (1); chemometrics.

What is most important from results of the current study is the next correlative analysis of experimental mass spectrometric and theoretical data on **equations (2) and (3)**, examining *molecular isotopologies* of loratadine (2). Let us look at experimental variables depicted and summarized in **Figure 18** and **Table 4**. It should be obvious from shown MS spectrum that, due to complexity of isotope shape employment in classical quantitative approaches to process data on MS measurands such as calculation of MS peak area should decrease crucially reliability of analytical information as a result from increasing in standard deviation of variables (see  $sd(yEr)$  parameters of **Table 4**.) Conversely, our stochastic dynamic approach and equation (2) processing MS variables *per* short span of scan time provide reliable results, despite, complexity of the shown isotope MS pattern. Due to, this reason chemometric assessment of relationship  $D''_{SD}=f(D_{QC})$  is characterized by excellent-to-exact method performances ( $|r|=0.99925$ ) (**Figure 19**.) The deviation of exact  $|r|=1$  parameter is a result from great dispersion of MS measurands (**Table 4**;) thus causing for quantifying variables having very close mean values, despite, the fact that are statistically significantly different.

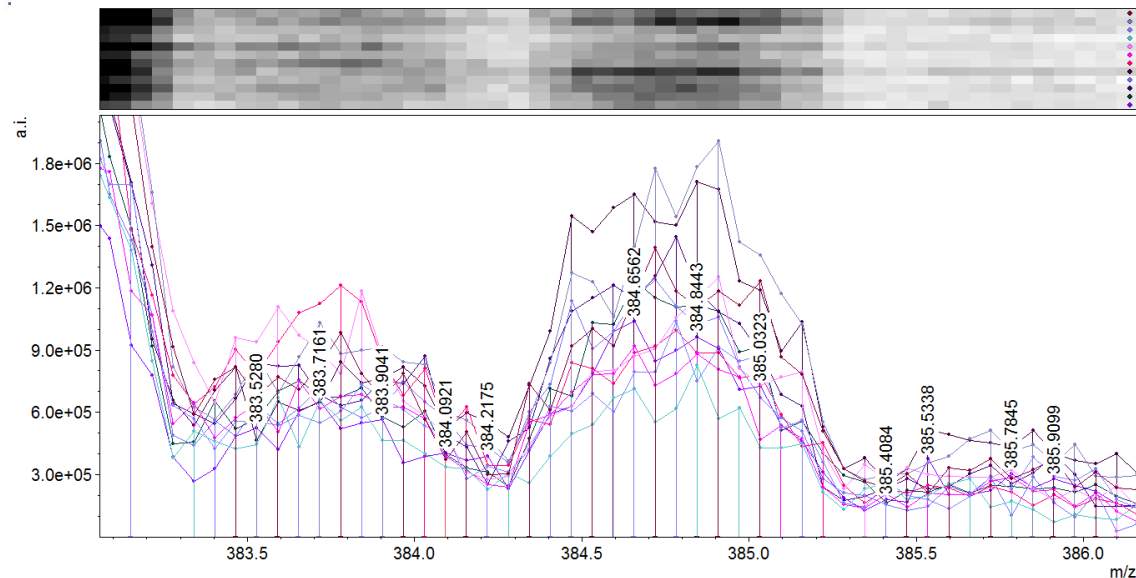


**Figure 18.** ESI-MS spectrum of loratadine (2) *per* span of scan time with respect to concentration of formic acid  $C_{FA} = 0$  M, and collision energy  $CE=50$  V.

Scan	m/z	I										
01	384.71893	1.39.10 <sup>5</sup>	385.03235	1.23.10 <sup>5</sup>	383.46533	821065.613	383.77869	984457.673	383.96674	789193.71	248.07336	34271.3789
02	384.71893	1.78.10 <sup>5</sup>	--	--	383.52802	876073.327	383.71606	1.03.10 <sup>5</sup>	383.90405	915113.401	-	-
03	384.78162	1.04.10 <sup>5</sup>	385.03235	875817.698	383.52802	559912.231	383.65338	588072.353	383.84137	736488.536	248.01071	42588.0848
04	384.96967	621377	385.15771	450065	383.5907	669889	383.71606	659521	383.84137	628865	248.19873	11381
05	384.90698	1.26.10 <sup>5</sup>	385.15771	795780.823	383.5907	1.11.10 <sup>5</sup>	-	-	383.84137	1.19.10 <sup>5</sup>	248.01071	24418.3919
06	384.8443	883137	385.09503	537793	383.52802	647233	383.65338	753025	383.84137	686529	248.01071	8369
07	384.78162	997404.644	385.03235	782748.685	383.46533	905116.429	383.77869	1.21.10 <sup>5</sup>	384.02942	813532.521	248.07336	61.33003
08	384.8443	1.71.10 <sup>5</sup>	385.15771	1.04.10 <sup>5</sup>	383.46533	819017.613	383.77869	843017.673	-	-	248.13605	19350.391
09	384.71893	1.24.10 <sup>5</sup>	-	-	-	-	383.71606	728449	-	-	248.01071	25146
10	384.78162	1.45.10 <sup>5</sup>	-	-	-	-	-	-	-	-	248.07336	25292
11	384.8443	1.12.10 <sup>5</sup>	385.15771	560513	-	-	-	-	-	-	248.26141	8987
12	384.8443	965313	385.03235	726337	-	-	-	-	-	-	248.07336	7440
Mean	384.81296	-	385.09503	-	383.52018	-	383.72388	-	383.8951	-	248.08477	-
sd(yEr±)	0.07793	-	0.06268	-	0.05231	-	0.05228	-	0.07616	-	0.08323	-
se(yEr±)	0.0225	-	0.02089	-	0.01849	-	0.01848	-	0.02879	-	0.0251	-
<I>	-	1.20.10 <sup>5</sup>	-	777662.562	-	800984.985	-	850312.568	-	822125.552	-	18845.8706
<I> <sup>2</sup>	-	1.45.10 <sup>12</sup>	-	6.05.10 <sup>11</sup>	-	6.42.10 <sup>11</sup>	-	7.23.10 <sup>11</sup>	-	6.76.10 <sup>11</sup>	-	3.55.10 <sup>8</sup>
<I <sup>2</sup> >	-	1.55.10 <sup>12</sup>	-	6.60.10 <sup>11</sup>	-	6.68.10 <sup>11</sup>	-	7.62.10 <sup>11</sup>	-	7.05.10 <sup>11</sup>	-	5.06.10 <sup>8</sup>
<I <sup>2</sup> >-<I> <sup>2</sup>	-	1.05.10 <sup>11</sup>	-	5.55.10 <sup>10</sup>	-	2.64.10 <sup>10</sup>	-	3.91.10 <sup>10</sup>	-	2.92.10 <sup>10</sup>	-	1.51.10 <sup>8</sup>
D <sub>SD</sub>	-	2.77.10 <sup>-8</sup>	-	1.47.10 <sup>-8</sup>	-	6.97.10 <sup>-7</sup>	-	1.03.10 <sup>-8</sup>	-	7.72.10 <sup>-7</sup>	-	3.98.10 <sup>-9</sup>

**Table 4**

Mass spectrometric measurands *per* span of scan time (m/z and intensity (I) [arb.units]) *per* scan number of loratadine (2) toward concentration of formic acid  $C_{FA} = 0$  M, and collision energy  $CE=50$  V (see **Figure 18**), used to calculate  $D''_{SD}$  parameters of equation (2) according to chemometric criteria on normality and method performances; parameters of equation (2); chemometrics

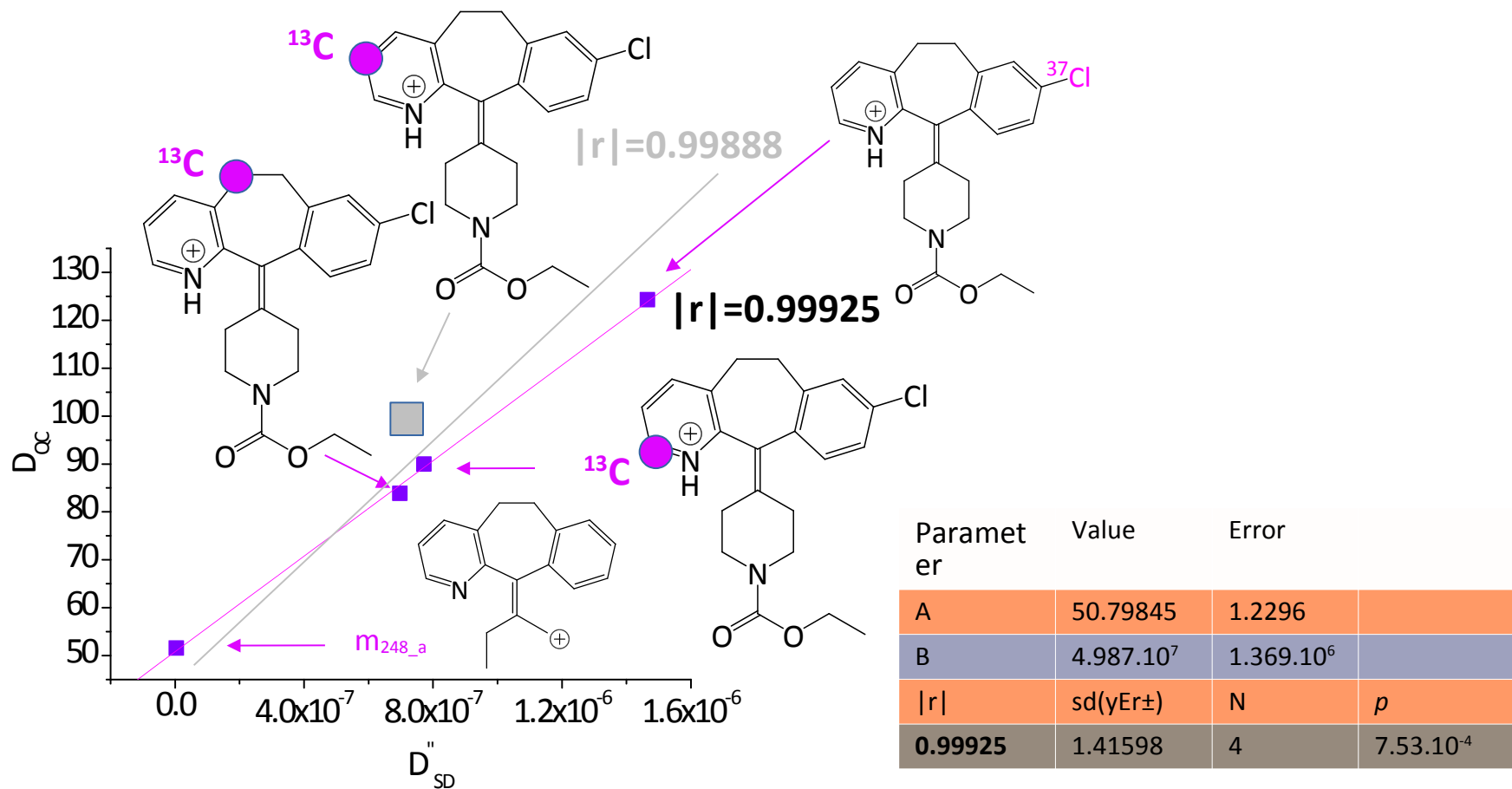


Figure 19. Correlative analysis between  $D''_{SD}$  and  $D_{\alpha C}$  data on equations (2) and (3) of MS fragmentation ions of analyte (2); chemometrics (see Tables 3 and 4).



## Conclusions

To sum up, looking at the results presented, herein, a general conclusion is obvious: The innovative stochastic dynamic model **equations (2), (4) and (5)** offer new perspectives for methodological developments of the *analytical mass spectrometry*; thus, underlying its both quantitative and 3D molecular structural analytical sub-fields. It emerges from application of formulas, so far, to problems of quantifying and determining 3D structurally pharmaceuticals in complex environmental and food samples as well as biological fluids, that equations provide exact quantitative and structural analyses from perspective of *chemometrics* ( $|r|=1$ ).

It seems highly relevant to examine systematically capability of the formulas, because of they make arguments in this study for universal application to the analytical practice, and determination about not only amount of a substance quantitatively and 3D molecular structurally, but also its molecular *isotopologies*. As the current contribution notes, application of equations (2), (4) and (5) to examine mass spectrometric measurands of diclofenac and loratadine has resulted to excellent-to-exact correlation coefficients between theory and experiment. Particularly, the relationship  $D''_{SD}=f(D_{QC})$  of examining **molecular isotopologies** of loratadine yields to excellent correlation coefficient  $|r|=|0.99925|$ , examining statistically representative set of fragmentation peaks of analyte (2). This is the second molecular example, highlighting persuasively the great prospect of application of equation (2) to quantify and determine 3D structurally fragmentation species exhibiting subtle electronic effects, including determining species, according to their isotopic specific positions of isotopes of atoms in a molecule. Therefore, this contribution highlights the prospective impact of **equation (2)** on the field of *isotomics*, among other interdisciplinary areas of application employing broadly *omics-methods*. Despite, the fact that, currently, there are conceptual difficulty to determine concentrations of individual molecular isotopologies of analyte mass spectrometrically, the results from this study underline clearly that further research effort devoted to this issue within the framework of innovative model equations presented, herein, are justifiable, due to reliability of data evaluated by methods of *statistics* and *chemometrics*.



# The 9th International Electronic Conference on Medicinal Chemistry

01-30 November 2023 | Online



## Acknowledgments

**DAAD**

Deutscher Akademischer Austausch Dienst  
German Academic Exchange Service



Stabilitätspakt für Südosteuropa  
Gefördert durch Deutschland  
Stability Pact for South Eastern Europe  
Sponsored by Germany

**DFG**

Deutsche  
Forschungsgemeinschaft

Alexander von Humboldt



Stiftung / Foundation